UNIVERSITIY OF CALIFORNIA SAN DIEGO

Conditional Deletion of NFIA Alters Motor Neuron Development

A thesis submitted in satisfaction of the requirements

for the degree Master of Science

in

Biology

by

Sara Abumeri

Committee in charge:

Professor Stacey Glasgow, Chair
Professor Brenda Bloodgood, Co-Chair
Professor Gulcin Pekkurnaz

2020

The Thesis of Sara Abumeri is approved, and it is acceptable in quality and form for publication on microfilm and electronically:

_____

_____

Co-Chair

_____

Chair

University of California San Diego

2020

TABLE OF CONTENTS

SIGNATURE PAGE.....iii

TABLE OF CONTENTS.....iv

LIST OF FIGURES.....v

LIST OF SCHEMATICS……..vi

LIST OF TABLES……...…….vii

LIST OF ABBREVIATIONS.....vii

DEDICATION.....ix

ABSTRACT OF THE THESIS.....x

INTRODUCTION.....1

MATERIALS AND METHODS.....14

RESULTS.....25

DISCUSSION.....34

FIGURES.....38

REFERENCES.....53

LIST OF FIGURES

FIGURE 1. Motor Neuron Column Organization in Embryonic Chick Spinal Cord Shows NFIA in MMC, LMC-m, and LMC-l MNs……...……...38

FIGURE 2. NFIA is Overexpressed in RCAS NFIA Spinal Cords and Knocked Down in RCAS NFIAi Spinal Cords. ……...…….40

FIGURE 3. Altered Expression of LIM1/2 and FOXP1 in NFIAi Spinal Cords.……41

FIGURE 4: Motor Neuron Column Organization in Embryonic Chick Spinal Cord Shows NFIA in MMC, LMC-m, LMC-l, and HMC MNs …….....43

FIGURE 5: Conditional Deletion of NFIA in HB9 CRE Neurons Leads to Reduced Expression and Migration of LIM1/2 and FOXP1……..45

FIGURE 6: Conditional Deletion of NFIA in ISL1 CRE Neurons Leads to Reduced Expression and Migration of LIM1/2 and FOXP1……..47

FIGURE 7: Reduction and Migration of FOXP2 in HB9 and ISL1 Transgenic Spinal Cords…….49

FIGURE 8: Reduction of PAX2 in $NFIA^{F/F}$;ISL1 CRE Spinal Cords……...……50

FIGURE 9: Wildtype Embryonic Motor Neurons Analyzed in Cell Culture…….....52

LIST OF SCHEMATICS

Schematic 1. Organization of the Spinal Cord and Motor Neuron Columns……..7

Schematic 2. Layers Observed in Motor Neuron Purification……..23

LIST OF TABLES

Table 1. Primary Antibodies used in Immunostaining Analysis ……..……...…….19

Table 2. Secondary Antibodies used in Immunostaining Analysis……...……....20

Table 3. Materials used in Motor Neuron Culture……....24

LIST OF ABBREVIATIONS

SC	Spinal Cord
MN	Motor Neuron

DEDICATION

I dedicate this to my parents and sisters. Their love, support, and encouragement mean everything.

I would like to thank my mentor, Dr. Stacey Glasgow. Stacey, I could not have completed this study without you. Over the past year, you have not only been a thoughtful, patient mentor, but a friend as well. Thank you for this experience.

I also thank Dr. Brenda Bloodgood and Dr. Gulcin Pekkurnaz for guiding me and being on my committee.

ABSTRACT OF THE THESIS

Conditional Deletion of NFIA Alters Motor Neuron Development

by

Sara Abumeri

Master of Science in Biology

University of California San Diego, 2020

Professor Stacey Glasgow, Chair

Professor Brenda Bloodgood, Co-Chair

Proper spinal cord development results in spatially organized motor columns that innervate muscles along the rostral-caudal body axis. This is achieved in large part through the concerted action of a combination of transcription factors. The transcription factor Nuclear Factor 1 A (NFIA) is a regulator of glial cell development where it is both necessary and sufficient to induce glial cell specification. NFIA is also expressed in developing neurons in the brain and in spinal motor neurons. Recently, differential expression of NFIA in spinal glial and motor neuron populations was found to depend on distinct chromatin architectures. However, the function of NFIA is motor neurons remains poorly understood.

Here, we show that NFIA is expressed in all but one motor column in developing spinal motor neurons. We define NFIA expression in both chick and mouse spinal cords, finding that

NFIA is expressed in MMC, HMC, LMCm, and LMCl columns. Using genetic manipulations in both chick and mouse spinal cord, we found that NFIA is not required for the initial specification of motor neuron populations. Rather, conditional deletion of NFIA in motor neurons leads to disorganization of the lateral medial motor neuron (LMC) columns. A reduction in expression and abhorrent migration of FOXP1 and LIM1/2 were observed with cells from the LMC-lateral column incorrectly migrating into the LMC-medial region. Thus, NFIA is important for maintain proper motor neuron columnar organization.

INTRODUCTION

NFIA is a known regulator of spinal glial cell development. NFIA is also expressed in spinal motor neurons, though its role remains unknown. We aim to define the role of NFIA in spinal cord development and ask if conditional deletion of NFIA impacts motor neuron specification, localization, and organization. Furthermore, we hope to gain a better understanding of NFIA's role in motor skill, motor disease progression, and motor neuron deterioration.

To introduce this study, I will define NFIA, the importance of glial cells, and glial cell development (1.1), NFIA and gliomas (1.2), motor neuron development and NFIA's expression (1.3), and define our research process to study motor neurons (1.4).

1.1 Nuclear Factor 1A and Glial Cells

The NFI family of transcription factors are involved in the development and functionality of the central nervous system. Members of the NFI family include NFIX, NFIB, NFIC, and NFIA. NFI family genes are found in various regions of the nervous system like the neocortex, spinal cord, cerebellum, and hippocampus (Gronostajski, 2002). They also have functions outside the central nervous system, in the pancreas and mammary glands. These genes are key factors in neural stem cell differentiation, strongly regulated during development, and important for maintaining gene expression during cell growth periods (Gronostajski, 2002). They are also implicated in axonal extension and guidance, glial and neuronal differentiation, and neuronal migration (Mason et al., 2009). Glial cells, astrocytes and oligodendrocytes, are the unsung heroes of the nervous

system. They make up more than half the cells in the brain and spinal cord and their role goes beyond. supporting neurons. Glia help with development, plasticity, and damage control within the nervous system (Zuchero and Barnes, 2015). Astrocytes are the most abundant type of glial cell. They aid neuronal survival, take up nutrients from blood to carry out metabolic processes, and help form a protective blood barrier around the brain (Zuchero and Barnes, 2015). Oligodendrocytes are needed to protect neurons, conduct signals, and myelinating axons of neurons in the central nervous system (Zuchero and Barnes, 2015).

Several studies have begun to elucidate the molecular mechanism that initiate glial cell development. The development of cells in the central nervous system begins with the production of neurons, or neurogenesis, starting between gestational days E9-11.5 in the mouse spinal cord. Deep projection neurons of the cortex will form first, followed by the superficial projection neurons (Bayraktar, 2015). As neurogenesis concludes, the production of glia, or gliogenesis, starts between E11-12.5. The transition from neurogenesis to gliogenesis is termed the "gliogenic switch." (Deneen et al., 2006). During this period, neurogenesis is inhibited, gliogenesis is activated, and glial cells are specified from radial glial cells that emerge from the embryonic neural tube and forebrain (Zuchero and Barnes, 2015).

NFIA, a member of the Nuclear Factor I Transcription Genes, functions during the gliogenic switch. NFIA is induced in the ventricular zone of the spinal cord (SC) as glial progenitors appear (Deneen et al., 2006). When NFIA is knocked down via siRNA spinal electroporation, expression of PAX6, OLIG2, AND SOX9 is reduced. These markers are ventricular zone (VZ) progenitor markers present during the gliogenic switch and are necessary to induce glial cell production. (Deneen et al., 2006). NFIA is necessary for the induction of glial cell progenitors and thus necessary for specification of glial identity during gliogenesis (Deneen et al.,

2006; Song et al, 2010). The expression of NFIA is regulated through a with a gliogenic chromatin looping mechanism that is formed prior to E10.5. This system is thought to govern precursors during glial development and is independent of the SOX9/BRN2 regulatory control (Glasgow et al., 2017). Together, SOX9 and BRN2 regulate NFIA's induction during the gliogenic switch in the developing VZ by utilizing a double looped chromatin structure, hence controlling NFIA's ability to drive forward gliogenesis (Glasgow et al., 2017). Upon its expression NFIA forms a complex that with Sox9 that induces the expression of subset of genes important for astrocyte identity (Kang et al., 2012).

Previous work on NFIA's role in central nervous system development has implicated its activity in transcriptional repression of gene induction and alteration of signal transduction pathways to decrease gene expression. Straight genetic knockout models in mice show the majority of mice lacking NFIA (95%) die shortly after birth due to breathing difficulties. The mice that do survive had neurological irregularities, like the inability to develop a corpus callosum, tremors, and cerebrospinal fluid build-up (Gronostajski, 2002). Interestingly, the four NFI genes may potentially help compensate for one another; when NFIA is deleted, defects can be partially compensated by the redundant role of another NFI gene (Gronostajski, 2002). Additionally, straight knockout of NFIA in the hippocampus of mice has a clear defect in cerebellar, spinal cord, and excretory system defects, suggesting NFIA plays a critical role in the health of the nervous system and beyond (Mason et al., 2009). Recent research found NFIA to be necessary for astrocyte function (Huang et al., 2020). Astrocytes with conditionally deleted NFIA in adult mice led to flawed astrocyte function in the hippocampus, causing deficits in neurotransmitter activity, impacted hippocampal circuits, inhibited long term potentiation, memory, and learning abilities, and loss of synaptic plasticity (Huang et al., 2020).

1.2 NFIA and Gliomas

Developmental pathways are reutilized in neurodegenerative diseases and malignancies. The most common forms of brain cancers are gliomas, which result from uncontrolled division of pathogenic astrocytes and oligodendrocytes (Glasgow et al., 2013). Gliomas can be categorized as astrocytoma's (stem from astrocyte cells), oligodendrogliomas (stem from oligodendrocyte cells), and glioblastomas (also stem from astrocyte cells) (Laug et al., 2018). NFIA is expressed differentially in astrocytomas and to a lesser extent in oligodendrogliomas (Song et al, 2010). The knockdown of NFIA disrupts gliogenesis and is necessary for the formation of malignant gliomas. Interestingly, NFIA's developmental relationships are maintained during gliomagenesis while it's inhibition of SOX10 can be manipulated to change the fate of glioma cells. Glasgow et al. found that overexpressing NFIA in the context of an oligodendroglioma can cause a conversion to an astrocytoma subtype of glioma. This reflects the ability of NFIA to not only drive astrogenesis during development but also in the tumor state (Glasgow et al., 2013).

Moreover, during glial development, miR-223, a small microRNA molecule can regulate NFIA expression. This relationship in maintained during gliomagenesis. Overexpression of miR-223 represses NFIA expression through a p21 mediated mechanism (Glasgow et al., 2013). p21 is a protein involved in cancer because it will halt the cell cycle to squash tumor formation (Abbas and Dutta, 2009). As tumors begin to develop, miR-223 reduces glial precursor proliferation by diminishing NFIA expression and strengthening p21 expression (Glasgow et al., 2013). There is a negative correlation between NFIA and gliomas. Furthermore, NFIA interacts with OLIG2 to repress p21, suggesting a rescue technique to prevent the proliferation of gliomas. (Kang et al., 2012; Glasgow et al., 2013).

1.3a Motor Neuron Development

The spinal motor neuron progenitor domain (pMN) gives rise to motor neurons in embryonic spinal cords. Motor neurons and glial cells are generated from the same region of the developing spinal cord, the pMN (Laug et al., 2018). Motor neurons are generated first from the pMN domain followed by glial progenitors that will give rise to glia (oligodendrocytes and astrocytes) (Ravanelli and Appel, 2015). After neurulation, retinoic acid (RA) will signal an increased expression of SHH by the notochord leads to release of GLI proteins (bifunctional glioma-associated oncogene transcription factors) (Stifani 2014). These GLI proteins work in tandem -- GLiA, an activator protein, and GLiR, a repressor protein controls the activity of Class I and Class II proteins (Stifani 2014). Class I factors DBX1, DBX2, IRX3, and PAX6 are induced by GLiR. Class II factors NKX6.1, NKX6.1, OLIG2, and NKX2.2 are induced by GLiA (Stifani 2014). The equilibrium of activation-inhibition creates distinct zones within the spinal cord that lead to the generation of five progenitor purviews: p0, p1, p2, pMN, and p3, each with a distinctive set of transcription factors and defined roles (Stifani 2014).

The pMN, is characterized by the grouped expression of NKX6.1, PAX6, and OLIG2 (Tanabe et al., 1998l; Stifani 2014). These factors ensure that motor neurons are generated and specified in the correct region of the spinal cord (Price and Briscoe, 2004). NEUROG2 is recruited as well and this factor promotes the expression of subsequential motor neuron (MN) genes (Stifani 2014). Interestingly, it is this harmonization between OLIG2 and NEUROG2 that controls the generation of MNs and oligodendrocytes from separate domains in the spinal cord (Lee et al., 2005; Stifani 2014). Lastly, a coordination of ISL1 and LHX3 is needed to induce cholinergic activity characteristics to spinal motor neurons (Stifani 2014). LHX3 is a LIM-homeobox gene

needed to promote both spinal motor neuron and interneuron generation (Thaler et la., 2002). During development of the spinal cord, LHX3 is inducted early on in the spine. ISL1 acts during development of motor neurons and is an early indicator of motor neuron differentiation (Pfaff et al., 1996). Once the development process is complete, the unique, amalgamated expression of transcription factors that inform the formation of the pMN domain and subsequent MN populations are organized into motor columns along the axis of the spinal cord (Stifani et al., 2014)

The spinal cord itself is divided into cervical, rostral (upper), thoracic (middle), caudal (lower) regions, and sacral regions. Rostral and caudal zones are anatomically identical, both innervated by the limbs, and known as the brachial/lumbar spinal cord subdivisions. Each region has lower motor neurons and is a medley of different cell types organized into singular columns (Stifani 2014). These columns are clusters of motor neurons that stretch along an axis from the rostral spine down to the caudal spinal cord. Furthermore, each column contains specific genes (Dasen et al., 2005; Stifani 2014).

The cervical region of the spinal cord has median motor (MMC), phrenic motor (PMC), and spinal accessory columns (SAC) (Schematic 1). The MMC axons project to the axial muscles and MMC MNs preserve posture of the spine. The PMC axons project and innervate the diaphragm and PMC MNs create a recurrent movement of muscles during inhalation and exhalation. The SAC axons target the mastoid and neck muscles and SAC MNs act as the link between the brain and cervical regions (Stifani 2014). The thoracic region of the spinal cord has MMC, hypaxial motor (HMC), and preganglionic motor columns (PGC) (Schematic 1) (Stifani 2014). The HMC axons project to the body wall and intercostal muscles and HMC MNs help preserve an organism's musculature. The PGC axons target sympathetic chain ganglia and PGC MNs coordinate the activity of smooth muscle and glands (Stifani 2014). The brachial/lumbar region has MMC, and

lateral motor columns (LMC) (Schematic 1). At the limb levels of the spinal cord, LMC MNs develop and are divided into the LMC-medial (LMC-m) and the LMC-lateral (LMC-l) column (Stifani 2014). LMC-m axons target the ventral limb region. LMC-l axons targets the dorsal limb region. The LMC is the primary MN column that innervates the limbs; without these medial and lateral columns, motor signaling, and muscular contraction could not occur properly (Stifani. 2014).

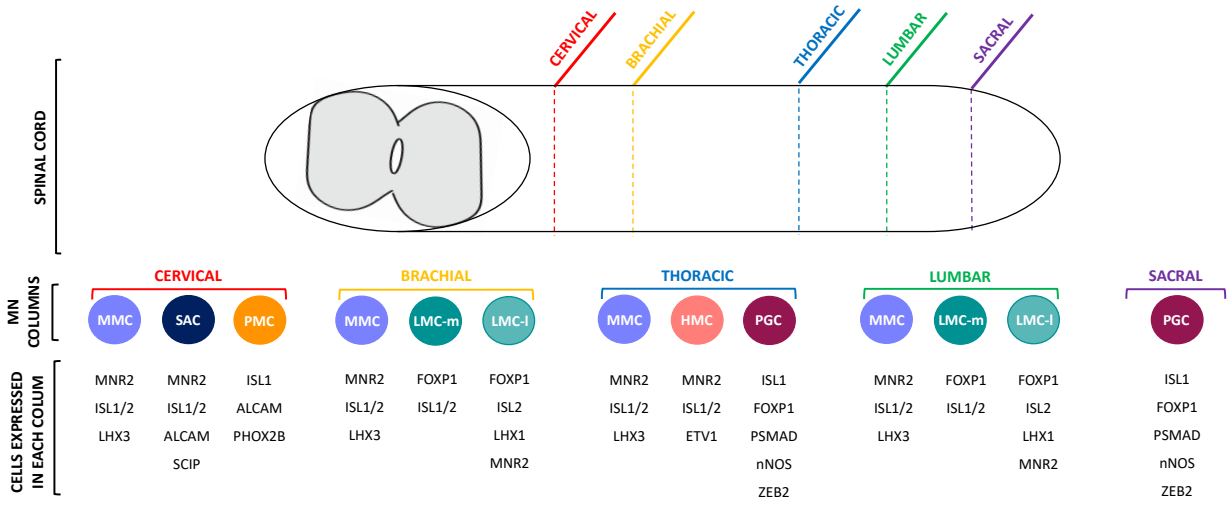

Schematic 1. Organization of the Spinal Cord and Motor Neuron Columns. Visualization of the spinal cord divided into cervical, brachial, thoracic, lumbar, and sacral regions. Each spinal cord region has corresponding MN columns. Each MN column has a corresponding unique genetic identity. This schematic has been modified based on images from Stifani 2014.

1.3.b FOXP1: Motor Neuron Identity

Forkhead Domain Transcription Factor FOXP1 is a critical protein seen across the nervous system, cardiac, and hemopoietic regions (Dasen et al., 2008). Previous studies have established FOXP1 as a critical player in spinal motor neuron development. FOXP1 acts jointly with HOX proteins to specify MN column identity and specification (Dasen et al., 2008). Secondly, FOXP1 expression is seen very early on in development in the LMC and PGC MNs. FOXP1 suppresses LHX3 in order to subdue MMC MNs and encourage specification of LMC and PGC MN identity

(Rousso et al., 2008). Furthermore, FOXP1 helps to organize axonal projections from these columns. FOXP1 is necessary to innervate distal limb muscles, which is the principal function of LMC-l MNs (Adams et al., 2015).

When FOXP1 is misexpressed, MMC MNs do not develop fully but LMC and PGC MNs are formed and their motor neuron pools are expanded (Rousso et al., 2008). Mouse models with conditionally deleted FOXP1 via FOXP1 mutant model with HB9::GFP reporter found LMC and PGC MNs develop incorrectly and have expression identities similar to MMC MNs. Interestingly, axonal projections from LMC MNs are still present, but there are more errors made in the axonal guidance to the limbs and reduced motor output (Rousso et al., 2008). Additionally, FOXP1 mutations lead to motor activity loss and nerve damage in the late stages of development, suggesting that misexpression seen in the early stages of development may have detrimental effects at a later time point (Rousso et al., 2008).

FOXP1 has also been linked to neurodegenerative diseases. FOXP1 is reduced in the striatum and cortex of patients suffering from Huntington's Disease (Titus et al., 2012). Moreover, FOXP1 is proposed to have a protective effect over neurons by stimulating expression of p21 (Titus et al., 2012). A separate study notes that axonal projections to the limbs are among the first to be impaired in neurodegenerative motor diseases, like Amyotrophic Lateral Sclerosis (ALS) (Adams et al., 2015). Being that FOXP1 is critical to LMC and PGC MN axonal trajectory to the limbs, the loss of this protein could be involved in ALS pathways as well.

1.3.c LIM1: Motor Neuron Identity

LIM Homeobox Protein 1 LIM1 (LHX1) is dominantly expressed in the central nervous system. ISL1 and LIM1, which act in conjunction with FOXP1, are critical for the segregation of cellular divisions within the LMC and for the specification of axonal targeting out of LMC MNs (Palmesino et al., 2010). In the initial formation of the LMC, both the medial and lateral columns express ISL1. As the motor neurons develop, ISL1 diminishes from LMC-l but stays in the LMC-m (Kania et al., 2000). LIM1 ensures the organization of LMC-l MNs by repressing expression of ISL1 (Kania et al., 2000). Additionally, LIM1 is needed for accurate axonal projections from LMC-l to the dorsal limbs, though without this gene, LMC-l cell specification proceeds as normal (Kania et al., 2000).

1.3d Mature Motor Neurons and Motor-Related Disorders

Mature motor neurons are classified as upper or lower motor neurons. Upper motor neurons extend from the primary motor cortex to the rest of the central nervous system. Lower motor neurons exist within the brainstem and spinal cord and also extend beyond the central nervous system to coordinate a muscle response (Stifani 2014).

Damage to upper neurons leads to reflex and movement issues. Diseases like sclerosis result from loss of function of upper motor neurons. Damage to this group of neurons can lead to severe paralysis and sensation issues (Stifani 2014). These lower MNs are further divided into three categories: brachial, visceral, and somatic. Brachial MNs coordinate activity in the brainstem and Visceral MNs coordinate activity of the autonomic nervous system (Stifani 2014). Somatic motor neurons govern our somatic nervous system and are further classified as alpha, beta, and gamma neurons (Stifani 2014). Alpha MNs project out into extrafusal muscle fibers and are

necessary for the function of muscle activity and contraction (Stifani 2014). Beta MNs are important for intrafusal and extrafusal fibers and aid in dispatching sensory feedback received from muscle spindles (Stifani 2014). Gamma MNs are not involved in the motor response and instead help in monitoring the sensitivity of our muscle spindles (Stifani 2014).

1.3e NFIA and the Chromatin Looping System

A study from 2017 began to investigate NFIA's role in the developing spinal cord. The motor neuron hexamer complex ISL1/LHX3 regulates development of spinal motor neurons and these two factors coordinate the activity of e96, a long range enhancer expressed in MNs (Glasgow et al., 2017). The expression of ISL1 and LHX3 is also necessary for normal NFIA expression as they regulate the induction of NFIA in MNs (Glasgow et al., 2017). Importantly, chromatin confirmation analysis techniques revealed lineage specific chromatin loops within the spinal cord that regulate expression of NFIA and induction of motor neuron precursors for motor neuron proliferation in glial and MN lineages (Glasgow et al., 2017). Given that NFIA is expressed in MNs and its regulation is mediated by a motor neuron complex, it will be important to determine what the downstream function of NFIA is MN development and function (Glasgow et al., 2017).

Prior research has established two concepts: One, NFIA is a critical transcription factor in glial development, regulates the gliogenic switch, and is involved in glioma proliferation (Deneen et al.,2006; Glasgow et al., 2013; Laug et al., 2018). Two, NFIA is expressed in spinal motor neurons. It's expression in motor neurons is regulated by a distinct chromatin looping mechanism than its expression in glial cells, which mechanisms drive these differential looping mechanisms have not been defined (Glasgow et al., 2017). Given NFIA's role in gene regulation and specification of spinal cord populations, we hypothesize that NFIA is important for motor neuron

development and will likely regulate motor neuron gene expression. In order to address the larger question of how NFIA is involved in the motor neuron development, we aim to examine the role of NFIA in developing spinal motor neurons using gain-and loss-of- function studies in both mouse and chick model systems.

In our first model, electroporation techniques were utilized in embryonic chicken spinal cords to overexpress or knockdown NFIA. To do this, replication-competent retroviruses (RCAS vectors) are used to transform gene expression (Hermann and Logan, 2003). RCAS-NFIA delivery overexpresses NFIA in the spinal cord. Small interfering RNA (siRNA) molecules are used in electroporation to transform gene expression of the host (Arabsolghar and Rasti, 2012). RCAS-NFIA-siRNA (RCAS NFIAi) delivery reduces NFIA expression in the spinal cord. RCAS was delivered alone as a control with fluorescent protein mCHERRY. After electroporation, chick spinal cords were collected at E5 and immunohistochemistry was used to verify the efficacy of the electroporation and analyze MN markers.

In our second model, NFIA was conditionally deleted in motor neuron subpopulations in the mouse spinal cord. HB9 and ISL1 cell lines were studied because NFIA is expressed in these cell lineages. HB9 is a homeobox gene that is necessary for motor neuron differentiation and migration (Arber et al., 1999). ISL1 is a transcription factor part of the LIM homeodomain. It is critical for motor neuron development, column growth, and motor neuron survival (Liang et al., 2011). Using a CRE-LOX system, NFIA was conditionally deleted in HB9 cells (an HB9 CRE $NFIA^{F/F}$ line) and ISL1 cells (an ISL1 CRE $NFIA^{F/F}$ line) creating the transgenic mice used in this experiment. We aimed to characterize spinal cord motor neurons in wildtype and NFIA conditional knockout mouse embryos collected between E10.5 and E18.5.

Additionally, we aimed to establish an embryonic spinal motor neuron culture technique. This culture system allowed us to harvest motor neurons from E14.5 embryos. Once motor neurons are grown in culture for at least five days, we used immunohistochemistry to analyze motor neuron cell presence, size, and shape from E14.5 mouse spinal cords. In future studies, we will employ this culture technique to study our transgenic mouse lines in order to further understand the impact of the loss of NFIA in live cells.

1.5b Purpose of this Study

We found that conditional deletion of NFIA in motor neurons leads to reduced expression of FOXP1 and LIM1/2. We saw the reduction of FOXP1 in the motor neuron pools and increased migration of these cells outside the MN columns. In addition to being reduced in number, LIM1/2 cells migrate out of the LMC-l and into the LMC-m motor columns in the absence of NFIA. These phenotypes are corroborated in the chick model system where we found that RNAi mediated deletion of NFIA has similar phenotypes to NIFA motor neuron conditional deletion. Therefore, we further hypothesize that NFIA is involved in the organization and specification of motor neuron columns.

The success of this research helps to build a comprehensive study about NFIA that can help identify the specific role NFIA plays in the motor neuron chromatin loop of the spinal cord. The ultimate goal of this project is to further our understanding about motor neuron physiology and degenerative and debilitative motor disease. There are several motor physiology diseases which have yet to see a cure. Explaining the role of transcription factors within the spinal cord illustrates how the spine is altered by gene presence. This could be instrumental in research geared toward

cures. The key to addressing problems that arise later in life begins by thoroughly examining an organism's development.

MATERIALS AND METHODS

Mouse Colony Housing and Breeding

All studies involving mice were approved by the Institutional Animal Care and Use Committee (IACUC) at the University of California, San Diego in accordance with NIH guidelines. Adult mice were housed one to five per cage, maintained on consistent food and water cycles, and materials for nesting and enrichment were supplied.

The breeding colony was maintained by interbreeding heterozygous mice and offspring were genotyped using PCR on tail DNA. Transgenic mouse lines included: $NFIA^{FF}$, $NFIA^{FF}$ x HB9 CRE, $NFIA^{FF}$ x HB9 CRE HB9 GFP, $NFIA^{F+}$ Td Tomato x $NFIA^{F+}$ ISL CRE, $NFIA^{FF}$ X ISL CRE, $NFIA^{FF}$ X ISL CRE HB9 GFP.

Timed Matings

Female mice were impregnated based on a timed mating schedule, with two female mice of the same genotype in a breeding cage with one male. Every morning between 7-10am, females were examined for a vaginal plug and if present, this day was marked as gestational day 0.5 (E0.5). The first day of birth was marked as postpartum day 0 (P0).

Females were harvested between gestational day 10.5-18.5. The female was euthanized, embryos were isolated, fixed in 4% PFA (4g PFA, 100ml 10xPBS, 75ul NAOH) for 1hr to overnight fixation (based on embryonic day), washed in PBS for 30 minutes, and left in 20% Sucrose (100g Sucrose, 500ml 10x PBS) overnight.

Embryos were embedded in an optimal cutting temperature (OCT) compound for sectioning via cryostat and spinal cord analysis. Embryos were separated based on rostral-caudal

location along the spinal cord: rostral, thoracic, and caudal. OCT embedded embryos were sectioned via cryostat onto glass slides and immunostained with various motor neuron markers.

PCR

Tail Tip DNA Extraction

Small tail pieces were collected during at the time of harvest. The tail tube was incubated in a solution containing: 50 mM NaOH and heated at 95oC in a heat block for 12 minutes. (50 mM NaOH is made with 1 g NaOH and 500 ml DI Water). Tubes were cooled at room temperature for 5 minutes. Tail samples were neutralized in buffer (30 ul 1M Tris (pH8), 5mM EDTA (pH8)). (1M Tris (pH8), 5mM EDTA (pH8) is made with 60.57g Tris, 5 mL 0.5 M EDTA pH 8, brought to a volume of 500 mL with DI Water, and the pH calibrated to 8 with 1 M HCL). Tails were then subjected to PCR genotyping or stored in a 4oC fridge for up to a year.

Genotyping

PCR was performed on genomic tail DNA preps to determine the presence of NFIA, ISL-CRE and HB9-CRE, and TDTOMATO.

For NFIA, the procedure is as follows: The reverse primer is A cNFIAdel-R (TGT GCG GCC TAC TCC AGA). The forward primer is E 12cc-F (CCG AGC ATG GAC GAC TTT GCT TTG). The master mix for the reaction was made accounting for each DNA sample with 6 ul EconoTaq Plus Green, 0.5 ul(uM) forward primer, 0.5ul(uM) reverse primer, 4ul water, and 1 ul DNA. Tail prep DNA was compared to control DNA preps for NFIA FF, NFIA F+, Wildtype, and Water. The PCR runs at (1) 95oC for 5 minutes, (2) 95oC for 30 seconds, (3) 55oC for 30 seconds, (4) 72oC for 30 seconds, (5) repeat 2-4, 35 times, (6) 72oC for 5 minutes, (7) 4oC until run on a

gel. The gel for this PCR is 2.5% agar and 1x Tris Acetate-EDTA (TAE) buffer and runs at a voltage of 115 mV for 45 minutes (TAE is made in a 50x stock solution with 50 mM EDTA, 2 M Tris, and 1 M Acetate)

For CRE, the procedure is as follows: The reverse primer is CRE Reverse (GGC GCG GCA ACA CCA TTT). The forward primer is CRE Forward (CCGGGCTGCCACGACCAA). The master mix for the reaction was made accounting for each DNA sample with 6 ul EconoTaq Plus Green, 1 ul (uM) forward primer, 1 ul (uM) reverse primer, 1 ul water, and 1 ul DNA. The sum samples included the various tailed tip DNA samples, the controls for CRE Positive (either ISL CRE or HB9 CRE), Wildtype, and Water. The PCR runs at (1) 94oC for 2 minutes, (2) 94oC for 30 seconds, (3) 59.5oC for 30 seconds, (4) 72oC for 40 seconds, (5) repeat 2-4, 28 times, (6) 72oC for 2 minutes, (7) 4oC until run on a gel. The gel for this PCR is 2.0% agar and 1xTAE and runs at a voltage of 115 mV for 45 minutes.

For TdTOMATO, the procedure is as follows: There are two reactions run. The first reaction, Wildtype, the reverse primer is ROSA WT-F (CAC TTG CTC TCC CAA AGT CG) and the forward primer is ROSA WT-R (TAG TCT AAC TCG CGA CAC TG). The second reaction, Td TOMATO Mutant, the reverse primer is ROSA-TdTOMATO-R (GTT ATC TAA CGC GGA ACT CC) and the forward primer is ROSA WT-R (TAG TCT AAC TCG CGA CAC TG). The master mix for each reaction was made accounting for each DNA sample with 6 ul EconoTaq Plus Green, 1 ul (uM) forward primer, 1 ul (uM) reverse primer, 1 ul water, and 2 ul DNA. The sum samples included the various tailed tip DNA samples, the controls for TdTOMATO positive, Wildtype, and Water. The PCR runs at (1) 95oC for 3 minutes, (2) 95oC for 30 seconds, (3) 59oC for 30 seconds, (4) 72oC for 30 seconds, (5) repeat 2-4, 40 times, (6) 72oC for 2 minutes, (7) 12oC

until run on a gel. The gel for this PCR is 2.5% agar and 1xTAE and runs at a voltage of 115 mV for 45 minutes.

Chick Electroporation

Eggs are received after fertilization from poultry service UC Davis campus and are placed to rotate in incubators with a temperature of 95oF for 3 days. Eggs are windowed for electroporation and marked as embryonic day 2. Only embryos that had developed to the proper E2 stage as determined by the Hamburger Hamilton staging were used for electroporation.

Electroporation plasmids are prepared at a final concentration of 1 ug/ul with DNA. Fast green dye was used to visualize DNA injection into the embryonic spinal lumen. Chick eggs were windowed and injected with plasmid via needle delivery to the spinal cord. The embryo was then treated with L-15 and penicillin-streptomycin solution and electroporated with 5 pulses delivered with 26 voltage for 50 milliseconds using a BTX electroporator.

Chick eggs were returned to the incubator and harvested at embryonic day 5. Embryos were washed with PBS, imaged for fluorescent protein if applicable, and decapitated, followed by fixation in 4% PFA (between 2-4hrs), and ultimately moved to sucrose overnight for overnight rotation. Embryos were embedded with OCT and sectioned via cryostat for immunostaining. Transgenic plasmids included: RCAS MCHERRY, RCAS NFIA RNAi, and RCAS NFIA.

Immunostaining Protocol/Imaging

Sections were washed with PBS 1x for 5-8 minutes. Water bath is set to 95o, a mailer is filled with 10 mls of Sodium Citrate Buffer and left in the water bath to preheat for 10 minutes (Sodium Citrate Buffer is made with 1L DI water, 2.94 g Tri-Sodium Citrate, 500 ul Tween20,

and pH is adjusted to 6.0). Slides immunostained for antibodies requiring antigen retrieval were incubated in sodium citrate mailers for varying times. After the incubation period, mailers were removed from the water bath and left to cool to room temperature (at least 15 minutes). Slides were then removed from the mailer and washed with PBS 3x for 5-8 minutes and incubated with appropriate blocking solution for 30mins-1hr. After blocking, primary antibody solutions (Table 1) containing the antibody and blocking solution were applied to slides and left to incubate in the 4o overnight. After incubation, slides were washed with PBS 3x for 5-8 minutes and incubated with appropriate secondary antibody solution (Table 2) for 1-2hr in the dark. The secondary antibody was prepared in a 1:500 dilution with the fluorescent antibody and blocking solution. Slides were then washed with PBS 2x for 5-8 minutes. DAPI was prepared in a 1:8000 dilution with PBS, added to slides, and left to incubate for 5 minutes. The slides were washed with PBS 1x for 5-8 minute and mounted with 50ul vectashield and coverslip and sealed with clear polish.

Coverslip Staining:

Coverslips were washed with PBS 1x for 5-8 minutes and then fixed with PFA for 10-15 minutes at room temperature. Coverslips were washed with PBS 3x for 5-8 minutes and incubated with appropriate blocking solution for 30mins-1hr. After blocking, primary antibody solutions (Table 1) containing the antibody and blocking solution were applied to coverslips and left to incubate in the 4o overnight. After incubation, coverslips were washed with PBS 3x for 5-8 minutes and incubated with appropriate secondary antibody solution (Table 2) for 1-2hr in the dark. The secondary antibody was prepared in a 1:500 dilution with the fluorescent antibody and blocking solution. Coverslips were then washed with PBS 2x for 5-8 minutes. DAPI was prepared in a 1:8000 dilution with PBS, added to coverslips, and left to incubate for 5 minutes. The slides

were washed with PBS 1x for 5-8 minute, mounted with 10 ul Vectashield, and sealed with clear polish.

Table 1. Primary Antibodies used in Immunostaining Analysis. Details of primary antibodies, their species, source company, skew #, and the concentration the antibody is prepared at with corresponding blocking solution.

Primary Antibody	Species	Company	Skew #	Conc.	Blocking Solution
NFIA	Rabbit	BD	N/A	1 : 2000	Goat / Donkey
NFIA	Guinea Pig	Thermofisher	N/A	1: 250	Goat / Donkey
FOXP1	Goat	R&D	AF4534	1 : 500	Donkey
FOXP1	Rabbit	Abcam	AB16645	1 : 2000	Goat / Donkey
ISL1/2	Mouse (IgG2b)	DSHB	39.4D5	1 : 25	Goat
ISL1	Goat	R&D	AF1837	1 : 50	Donkey
ISL1	Rabbit	Abcam	AB20670	1 : 400	Goat / Donkey
LHX3	Mouse (IgG1)	DSHB	6.74 e 12	1 : 5	Goat
LHX3	Rabbit	Abcam	AB124697	1 : 400	Goat / Donkey
TUJ1	Mouse (IgG2a)	Covance	MMS435P	1 : 100	Goat / Donkey
LIM1/2	Mouse (IgG1)	DSHB	4F2	1 : 5	Goat
GFAP	Mouse (IgG1)	Chemicon	MAB360	1 : 1000	Goat / Donkey
CHAT	Goat	Millipore	AB144P	1 : 100	Donkey
MNR2	Mouse (IgG1)	DSHB	81.5c10	1 : 10	Goat / Donkey
HB9	Mouse (IgG1)	SCBT	SC-515769	1 : 50	Goat
FOXP2	Rabbit	Abcam	AB16046	1 : 2000	Goat / Donkey
CHX10	Mouse (IgG2a)	SCBT	SC-365519	1 : 50	Goat / Donkey
PAX2	Rabbit	Thermofisher	71-6000	1 : 500	Goat / Donkey

Table 2: Primary Antibodies used in Immunostaining Analysis. Details of secondary antibodies, their species, source company, skew #, and the concentration the antibody is prepared at with corresponding blocking solution.

Secondary Antibody	Species	Company	Skew	Dilution	Blocking
ALEXA FLUOR 568	Goat Anti-Rabbit	Invitrogen	A-11036	1 : 500	Goat
ALEXA FLUOR 568	Goat Anti-Mouse	Invitrogen	A-11031	1 : 500	Goat
ALEXA FLUOR 568	Donkey Anti-Goat	Invitrogen	A-11057	1 : 500	Donkey
ALEXA FLUOR 488	Donkey Anti-Goat	Invitrogen	A-11055	1 : 500	Donkey
ALEXA FLUOR 488	Goat Anti-Rabbit	Invitrogen	A-11034	1 : 500	Goat
ALEXA FLUOR 488	Goat Anti-Mouse	Invitrogen	A-11029	1 : 500	Goat
ALEXA FLUOR 647	Donkey Anti-Goat	Invitrogen	A-21447	1 : 500	Donkey
ALEXA FLUOR 647	Goat Anti-Rabbit	Invitrogen	A-21245	1 : 500	Goat
ALEXA FLUOR 647	Goat Anti-Mouse	Invitrogen	A-21236	1 : 500	Goat

Motor Neuron Cultures

Embryonic

Our embryonic motor neuron culture system was adapted from the Beaudet et al., 2015 protocol.

(1) Embryo Extraction: Female mice were impregnated based on a timed mating schedule, with two female mice of the same genotype in a breeding cage with one male. The wildtype (WT) female crossed with a WT male. Females were harvested on gestational day 14.5. The mother was euthanized, the abdomen was opened with sterile instruments (all instruments used in this experiment are previously autoclaved at 135oC and 30 PSI for a 20 minute cycle), and the uterus was removed and transferred to a petri dish with 10 mls Lebovitz's Medium 15 (L-15) and Penicillin/Streptomycin (P/S) (Table 3; prepared with L-15 and 1% P/S). Embryos were removed

from the embryonic sack and the embryo's head and tissue surrounding the spinal cord was removed. The spinal cord was then further isolated from the dorsal root ganglions, meninges, and ribs, and cut into several small pieces. Harvested pieces were placed in 1ml of L-15/P/S in a six-well plate. Each spinal cord was isolated separately and placed into a corresponding well with medium.

(2) Cell Extraction: Isolated embryonic mouse spinal cords were processed to extract cells. Papain Working Solution (PWS) was warmed for 10-15 minutes in a 37oC water bath (Table 3; 1 ml PWS is prepared per spinal cord with 2 mg/ml papain, 40% L-15/P/S, and 60% 1x HBSS). After warming, isolated embryonic spinal cord pieces were removed from the six-well plate and added to 1ml PWS in a corresponding Eppendorf tube. The spinal cords were incubated in a 37oC chamber for 25 minutes, with the tubes manually rotated for 10 seconds every 5 minutes. During the last few minutes of the incubation, 5 ml of cold L-15/P/S was added to a 40 um cell strainer on top of a 50 ml collection tube. Spinal cords were removed from the incubator and collected from the Eppendorf tubes to a corresponding six-well plate. 3 ml of cold L-15/P/S were added to each well. The spinal cord and medium mixture were manually passed up and down via a glass pipette to further break down the tissue (no more than 6 times). The medium containing dissociated cells was collected from the well and poured through the cell strainer/50 ml tube. Another 4 ml of cold L-15/P/S was added to the remaining partially dissociated spinal cord tissue in the well for another round of titration. The media was collected and poured through the cell strainer/50 ml tube. Another 2 ml of cold L-15/P/S was added to the remaining partially dissociated spinal cord tissue in the well, titrated, collected, and poured through the cell strainer/50 ml tube. The cell strainer was washed with 3 ml of cold L-15/P/S and the 50 ml collection tube was inverted 6 times. Then,

the collection tube was centrifuged at 4oC and 280g for 10 min in a swinging bucket centrifuge. The centrifuge was repeated once more, and a white pellet composed of motor neurons formed.

(3) Motor Neuron Purification: The supernatant was removed from the collection tube and 1 ml cold L-15/P/S was added to the pellet containing motor neurons. The pellet was then resuspended by homogenizing with a glass pipette. Once resuspended, 5 ml of L-15/P/S was added to the collection tube. The medium in the collection tube was carefully layered on the surface of the previously prepared lymphocyte density solution via the glass pipette (Table 3; the Lymphocyte Density Solution is prepared at a volume of 10 mls at 1.077 g/ml with 9.84 ml of the density solution and 0.16 ml of L-15/P/S). This gradient solution was centrifuged at 900g using a swinging bucket centrifuge at 4oC for 20 min. After centrifugation, the gradient tube separates into three layers: a white pellet with small gamma motor neurons and astrocytes (LAYER 1), an interface with motor neurons, and a pink top layer with the L-15/P/S and cell debris (LAYER 2) (Schematic 2). The interface was collected with a 10 ml glass pipette and moved to a new 50 ml purification tube per genotype. The purification tube's volume was completed to 50 ml with cold L-15/P/S and centrifuged at 425g using a swinging bucket centrifuge for 10 min at 4°C. The supernatant was removed, and the motor neurons were resuspended in Motor Neuron Culture Medium. To make the Motor Neuron Culture Medium (MNCM), a DMEM Medium and Neurobasal A Medium were supplemented and mixed at a 1:1 ratio (To make DMEM Supplemented Medium: 100 ml DMEM medium, 36.54 mM $NaHCO_3$, 0.18 mM L-adenine, 312.5 u/L 2N HCL, 10% Fetal Calf Serum, 25 ug/ml pen-gentamicin. To make Neurobasal A Supplemented Medium: 1% B-27, 0.24 mM L-glutamine, 0.2 ug/ml hydrocortisone, 2.5 ug/ml insulin, 10 ng/ml NT3, 10 ng/ml GDNF, 10 ng/ml BDNF, 25 ng/ml CNTF). The cells were counted with a hemocytometer and plated at a density of 150,000 cells per well in a 24 well plate with glass

coverslips. One day prior to the start of the culture protocol, the wells of a 24-well sterile culture plate were covered with 12 mm diameter glass cover slips and coated with 0.5 mL of Poly-D-Lysine (PDL) (PDL is prepared with 5mg PDL and 50 ml sterile cell culture water) and left overnight in the laminar flow hood. On the day of the culture, the PDL was removed from the wells, wells were washed with sterile water twice and allowed to dry for 1 hr at room temperature, wells were coated with laminin 10 μg/μL in 350 μL MNCM and left for 2 hr at room temperature. Prior to plating the cells, the laminin was removed, and the wells were washed twice with sterile cell culture water. The cells were plated. For 30 minutes, only 100 ul of the cell suspension were plated and the 24 well plate was left in the 37oC incubation chamber so the cells could attach to the coverslips. Then, 2 mls of MNCM were added to the plate in order to feed the cells. After staying in the 37oC incubation chamber for 1 day, CAF was added to each well. Every two days 75% of the MNCM was removed and fresh MNCM was added. This process continues until coverslips are collected for analysis.

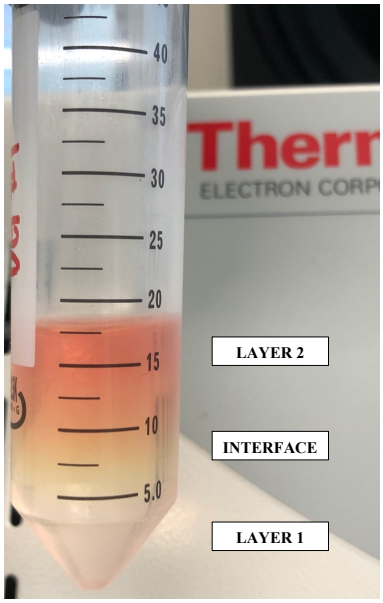

Schematic 2: Layers Observed in Motor Neuron Purification. Layer 1 contains gamma motor neurons and astrocytes. The Interface contains motor neurons. Layer 2 contains cell debris and L-15/P/S media.

Table 3. Materials used in Motor Neuron Culture. Details the list of reagents needed for this culturing system, their source company, and skew number.

Product Name	Company	Skew #
DMEM / F12	Life Technologies	11320082
Neurobasal A (w/o phenol red)	Fisher	12349015
Lymphocyte Separation Medium 1077	Promocell	C-440010
B27 Supplement	Fisher	17504044
Papain (lyophilized)	Fisher	NC9913764
Poly D Lysine	Sigma	P6407-5MG
Insulin	Sigma	I1882-100MG
Cytosine ß-D-Arabinofuranoside Hydrochloride	Sigma	C6645-100MG
L-Glutamine	Fisher	21051024
L-Adenine	Fisher	AVC147440250
Penicillin G Sodium Salt	Sigma	P3032-10MU
Hydrocortisone (Chroma)	VWR	80058-206
HBSS	Fisher	14185052
Leibowitz's 15	VWR	45000-372
GDNF	Biolegend	711002
BDNF	Fisher	50812764
CNTF	Biolegend	559802
NT3	Fisher	PHC7036
Hydrochloric Acid	Fisher	SA431500
Sterile Cell Culture Water	VWR	45000-672
PBS	Life Tech	10010049
Laminin Mouse Protein	Life Tech	23017015

RESULTS

RCAS NFIAi Knockdown Disrupts FOXP1 and LIM1/2 Expression in Motor Neurons

Previously, NFIA was shown to be expressed in the ventricular zone and motor neuron pools of the developing spinal cord. To define NFIA's expression in developing motor neurons, we used immunohistochemical analysis (IHC) in wildtype chick spinal cords. Using this method, we aimed to establish the transcriptional identity of MN columns and analyze NFIA in relation to existing MN markers. Our analysis of chicken spinal cords was localized to brachial/lumbar regions where MMC, LMC-m, and LMC-l MN columns exist. FOXP1 and MNR2 IHC co-staining analysis shows FOXP1 in LMC-m and LMC-l and MNR2 in the MMC and LMC-l (Fig. 1A). ISL1 and LIM1/2 co-staining shows ISL1 in the MMC and LMC-m and LIM1/2 in LMC-l (Fig. 1B). FOXP1 and ISL2 co-staining shows ISL2 in the MMC, LMC-m, and LMC-l (Fig. 1C). ISL1 and LHX3 co-staining shows LHX3 in the MMC (Fig. 1D). NFIA and MNR2 co-staining shows NFIA in the MMC, LMC-l, and LMC-m (Fig. 1E). These results establish NFIA within all three MN columns on the brachial level, meaning NFIA colocalizes with all examined MN markers.

To determine if NFIA is sufficient and/or necessary to influence spinal motor neuron specification, chicken spinal cords were subjected to gain-and loss-of-function studies *in ovo* electroporation at E2 and harvested at time points after specification. CMV-mCHERRY was delivered as an electroporation control. The presence of fluorescent reporter mCHERRY serves as an indicator of successful electroporation and IHC analysis of NFIA in these control embryos serves a baseline of NFIA expression in the chick spinal cord (Fig. 2A). NFIA was overexpressed using the chick RCAS expression vector system in the spinal cord (Fig. 2B). NFIA RNAi knockdown was mediated by the RCAS-NFIAi construct which was delivered to the spinal cord

(Fig. 2C). AMV staining, which marks viral proteins, confirmed expression of the plasmids by displaying strong fluorescence on the left side of the spinal cord where cells have been electroporated with RCAS vectors. The right side of the embryo serves as an internal "control" within the electroporation experiment. However, AMV appears to cross over the ventricular zone of the spinal cord from the EP side to the control, suggesting the there is some leakiness in expression to the other side of the spinal cord. This could explain variance in quantification or more modest differences between the electroporated and the unelectroporated sides (Fig. 1B, C). Analysis of NFIA in our control model versus mutant models demonstrates a significant increase in NFIA in the RCAS-NFIA model and a significant decrease of NFIA in the RCAS-NFIAi model (Fig. 1D). Together, these data demonstrate that we have the tools available to address the function of NFIA in the chick system.

Overexpression of NFIA did not result in any significant changes in MN markers as compared to the control, suggesting NFIA is not sufficient for MN specification, MN organization, or localization. Conversely, RNAi-mediated knockdown of NFIA resulted in significant disorganization of motor columns. In control spinal cords, LIM1/2 and ISL1 co-staining establishes separation of MN columns and demonstrates that ISL1 and LIM1/2 colocalization does not occur (Fig. 3A, B). However, LIM1/2 and ISL1 expression does overlap in RCAS-NFIAi spinal cords. The total number of ISL1 cells are not changed by the knockdown of NFIA, however LIM1/2+ cells appear to migrate out of the LMC-l into LMC-m and MMC MN pools, as evident by the increase in overlapping ISL1+ and LIM1/2+ cells in MN pools (Fig. 3B, E). Additionally, we see decreased number of LIM1/2 in the spinal cord as a whole (Fig. 3A, E). To determine if this reduction of LIM1/2+ cells is due to cell death, we analyzed Caspase3 via IHC. Analysis shows there was not a significant visual or quantitative increase Caspase3+ cells in RCAS-NFIAi

spinal cords (Fig. 3G, H). Further analysis of FOXP1 and ISL2 costaining in our controls verified published reports, finding colocalization of these markers in the LMC-m and LMC-l MN pools (Fig. 3C, D). However, while ISL2 was unaltered in our knockdown experiments, FOXP1 expression was altered. Interestingly, FOXP1 expression is reduced in LMC-m and LMC-l MN pools and there is less colocalization of FOXP1 with ISL2 (Fig. 3C, F). Again, after evaluating whether or not cell death was increased in RCAS-NFIAi spinal cords, we found no significant increase in CASPASE3 (Fig. 3G, H). Overall, knockdown of NFIA leads to reduction of FOXP1 and LIM1/2 expression and aberrant migration of LIM1/2 in LMC-m/l MN pools, suggesting NFIA is necessary for MN column organization.

Motor Neuron-Specific Deletion of NFIA leads to Motor Column Disorganization

To determine the function of NFIA in mouse motor neuron development, we first analyzed the expression of NFIA in developing mouse spinal cord. Similar to our results obtained in chick spinal cord, ISL1is found in the MMC and LMC-m motor pools and FOXP1 in LMC-m and LMC-l pools. (Fig. 4A). ISL1/2 and LHX3 co-staining verified that ISL1/2 is expressed in the MMC, LMC-m, and LMC-l and LHX3is expressed in the MMC (Fig. 4B). ISL1 and LIM1/2 co-staining shows LIM1/2 in LMC-l (Fig. 4C). NFIA and HB9 co-staining shows NFIA in the MMC, LMC-l, and LMC-m and HB9 in the MMC and LMC-l (Fig. 4D). We found NFIA cell expression patterns in wildtype mice to be identical to wildtype chick spinal cords. These results determine NFIA within all three MN columns on the brachial/lumbar level, meaning NFIA colocalizes with all studied MN markers.

In the thoracic region of the spinal cord, ISL1 and FOXP1 co-staining found ISL1 in the MMC, HMC, and PGC and FOXP1 in the PGC only (Fig. 4E). ISL1/2 and LHX3 co-staining

shows ISL1/2 in the MMC and HMC, only ISL1 in the PGC, and LHX3 in the MMC (Fig. 4F). ISL1 and LIM1/2 co-staining found LIM1/2 in no MN columns in this level of the spinal cord (Fig. 4G). NFIA and HB9 co-staining found both markers in the MMC and HMC (Fig. 4H). Our thoracic analysis demonstrates that NFIA is excluded from the PGC motor neuron column.

Having an established baseline of NFIA expression in wildtype spinal cord MNs, we developed transgenic mouse lines for conditional deletion of NFIA. The first line used a CRE-LOX system to target NFIA in HB9-expressing MNs. This will delete NFIA in the MMC and LMC-l MNs of the brachial/lumbar level and MMC and HMC MNs of the thoracic level. In establishing our model, we crossed an $NFIA^{FF}$;HB9-CRE male with and $NFIA^{FF}$;Td-Tomato female generating a pregnant female from which we harvested embryos at E12.5 (Fig. 5A). Embryos expressing $NFIA^{FF}$;HB9-CRE TD Tomato genotyping were fixed, embedded, sectioned, and immunostained for NFIA and Td-Tomato. We found Td-Tomato expression where HB9 MNs are expressed, confirming that our CRE line was working correctly (Fig. 5B). Furthermore, we compared HB9 and NFIA in control spinal cords to $NFIA^{FF}$;HB9-CRE spinal cords. As HB9 cells are not expressed in every MN column, we did not see full deletion of NFIA from MN columns. Instead, we saw consistent decreased expression of NFIA in all MN columns HB9 is expressed in. There is consistently 30-40% less NFIA cells in our transgenic line as compared to the control and less colocalizing between NFIA and HB9 cells in our conditional deletion model (Fig. 5C, D).

Our initial studies analyzed E10.5 and E11.5 spinal cords, as these are the time points where MN specification occurs. We found no significant differences in the markers analyzed. Therefore, we believe NFIA is not required for the formation of MNs in the developing spinal cord. Learning this, we asked whether or not NFIA was important for MN column organization and survival. Our first finding in $NFIA^{FF}$;HB9-CRE mice was a reduction of LIM1/2 cells in the brachial/lumbar

region of E13.5 mouse spinal cords. We additionally saw increased migration of LIM1/2 from LMC-m MNs. Co-staining of ISL1 and LIM1/2 in control spinal cords shows a clear delineation of the LMC-m and LMC-l MNs; ISL1 cells express in LMC-m MNs and LIM1/2 cells express in LMC-l MNs (Fig. 5E). In our conditional knockdown model, ISL1 is conserved but LIM1/2 cells migrate from the LMC-l into the LMC-m, colocalizing with ISL1 cells to a greater extent (Fig. 5F). Due to this migration, we found greater increase in co-labeled LIM1/2/ISL1 cells (Fig. 5I). Interestingly, we found reduction of LIM1/2 cells in transgenic HB9 spinal cords overall (Fig. 5I). This reduction looks to be primarily occurring in ventral and dorsal regions outside the MNs. We plan to further explore this reduction using dorsal transgenic mouse lines.

Our second finding in HB9 transgenic mice was a reduction of FOXP1 cells in the brachial/lumbar regions of the spinal cord, starting with embryos harvested at E13.5. Furthermore, we also observed increased migration of FOXP1 cells out of the MN pools. Co-staining of ISL1 and FOXP1 in control spinal cords demonstrated colocalizing of both markers in the LMC-m. In our $NFIA^{FF}$;HB9-CRE mice, ISL1 is conserved but we found clear reduction of FOXP1 cells in both the LMC-m and LMC-l (Fig. 5G, H). This reduction is clearly observed when analyzing the colocalization of FOXP1/ISL1. There are significantly fewer overlapping cells in our HB9 transgenic line (Fig. 5H, J). Furthermore, we found a novel phenotype with the migration of FOXP1 cells. As the presence of FOXP1 significantly diminishes in MN pools, there is a meaningful increase in the FOXP1 cells migrating from the MNs to the dorsal and ventral regions of the spinal cord (Fig. 5H, K). The reduction and disorganization of FOXP1 is also seen in E16.5 and E18.5 spinal cords, suggesting this phenotype is preserved after the E13.5 timepoint (Fig. 5N O)

Upon discovering the altered expression of LIM1/2 and FOXP1 in our transgenic HB9 line, we asked if the decrease in these MN markers lead to an increase in cell death. IHC analysis of Caspase3 in our control and mutant model demonstrates there is no significant increase in cell death (Fig. 5L, M). Overall, we found reduction, migration, and disorganization of FOXP1 and LIM1/2 in the brachial/lumbar levels of transgenic HB9 spinal cords. At the thoracic level of the spinal cord, no phenotype was observed.

Because NFIA is expressed in MNs outside of HB9 expressing MN populations we used a second motor neuron CRE-driver, Isl1-CRE. Interestingly, the results of Fig. 5 were mirrored in the second transgenic mice line used in this study. In establishing our model, we crossed an $NFIA^{F+}$;ISL-CRE male with and NFIA FF TD Tomato female generating a pregnant female from which we harvested embryos at E12.5 (Fig. 6A). Embryos expressing $NFIA^{FF}$;ISL1-CRE TD Tomato genotyping were fixed, embedded, sectioned, and immunostained for NFIA and Td-Tomato. We found Td-Tomato expression where ISL1 MNs are expressed (Fig. 6B). When comparing ISL1 and NFIA IHC in control spinal cords to our transgenic ISL1 spinal cords, we found that NFIA expression is not only knocked out in ISL1 MNs, but also in the ventricular zone of the spinal cord (Fig. 6C, D). This full knockdown lead to two notable findings.

Our first finding in the $NFIA^{FF}$;ISL1-CRE line was a decrease and migration of LIM1/2 cells starting in E13.5 mice. As observed with the $NFIA^{FF}$;HB9-CRE model, we found LIM1/2 cells migrating from the LMC-l and amalgamating with ISL1 cells in the LMC-m (Fig. 6E, F). In addition to migration, we again saw a reduction of LIM1/2 cells in the dorsal region of the spinal cord (Fig. 6F, I). Our second finding in this ISL1 line was a reduction and migration of FOXP1 cells starting in E13.5 spinal cords. This finding was also observed in the $NFIA^{FF}$;HB9-CRE line. We saw decreased expression of FOXP1 in LMC-m and LMC-l MNs and increased migration of

FOXP1 out of MN pools and into the dorsal and ventricular zone of the spinal cord (Fig. 6G, H, J, K). This phenotype is likewise preserved in later developmental stages E16.5 and E18.5 (Fig. 6N, O). Again, all phenotypes were seen at the brachial/lumbar level while MN expression was conserved in the thoracic region of our transgenic mice. After detecting LIM1/2 and FOXP1 disorganization, we analyzed Caspase3 cell presence but found no significant increase in cell death in our transgenic model as compared to the control (Fig. 6L, M).

Overall, both HB9 and ISL1 transgenic mouse lines see altered expression of LIM1/2 and FOXP1 at the brachial/lumbar level suggesting that NFIA is necessary for organization and normal expression of the LMC markers.

Alternated Expression of FOXP2 in Mice with Conditionally Deleted NFIA and Reduced PAX2 Expression in NFIA^{FF};ISL1-CRE Mice

After we conducted our analysis of MN markers in our transgenic mouse lines, we set out to uncover whether or not NFIA's expression is necessary for ventral cells of the spinal cord. We studied expression of Chx10 and FOXP2 in E12.5 and E13.5 spinal cords. IHC done on controls demonstrated Chx10 expression in V2 regions and FOXP2 in V1 regions of the spinal cord (Fig. 7A-C). Interestingly, in our ISL1 transgenic line, Chx10 expression is conserved but FOXP2 expression is slightly diminished and cells appear to migrate out of V1 domains. Moreover, there is increased overlapping cell expression in NFIA^{FF};ISL1-CRE mice (Fig. 7D-G). FOXP2 reduction and migration was also seen in our HB9 transgenic line, however, these mice seem to have even less FOXP2 as compared to the control and NFIA^{FF};ISL1-CRE spinal cords and even more sporadic disorganization (Fig. 7D-G). Whether the motor neuron domain in the spinal cord is

expanded or not in these conditional knockouts has not been determined and further analysis is needed to determine if spinal population boundaries are being affected in these mice.

Since ISL1 is also expressed in the dorsal interneuron population dI3 and NFIA^{FF};ISL1-CRE mice appear to have a complete spinal cord deletion of NFIA, we analyzed dorsal markers. We studied expression of PAX2 in E12.5 and E13.5 spinal cords. PAX2 and LIM1/2 IHC analysis was done in control and mutant mouse lines. Our controls established the expression of PAX2 in dl4, dlLa, and dl6 (only in E13.5) pools and LIM1/2 in dl2, dl4, dlLa, and dl6 (only in E13.5) pools (Fig. 8A-C). Conversely, PAX2 is significantly reduced in NFIA^{FF};ISL1-CRE spinal cords but not in NFIA^{FF};HB9-CRE spinal cords (Fig. 8D-G). Furthermore, there is significantly less overlapping expression of PAX2 and LIM1/2 in NFIA^{FF};ISL1-CRE spinal cords (Fig. 8D-G). As seen in the MN analysis, LIM1/2 expression is again reduced at E13.5 only (Fig. 8F). Overall, only our NFIA^{FF};ISL1-CRE line leads to altered expression of PAX2 in dorsal pools. We aim to further understand this finding with more mouse and chick analysis, new transgenic lines, and a culturing system.

Conformation of Embryonic Motor Neuron Cell Culture System

The findings in this study pertain to IHC analysis of chicken and mouse spinal cords. Going forward, we aim to use an *in vitro* motor neuron cell culture technique to expand our analysis. To begin, we established an embryonic motor neuron culturing protocol (Fig. 9). Embryos were collected from E14.5 wildtype pregnant mice and the motor neurons were collected from the spinal cord and grown in culture in a 24 well plate. Within the first 24 hours of culture, we treated each well with CAF, a glial cell growth inhibitor, to promote motor neuron cell growth. The media of each well is changed every 2 days, and coverslips were harvested on days 5 and 8 of the experiment

(Fig. 9A). To test the efficacy of this technique, IHC analysis of CHAT, LHX3, NFIA, ISL1, FOXP1, and TUJ1 was done for the two time points (Fig. 9B-I). Cells were counted, and marker expression increased between days five and eight (Fig. 9J). Overall, we established a culturing system which will be used in future studies to explore the findings of this thesis.

DISUCSSION

Summary of Analysis

Previous research establishes NFIA as a key regulator in gliogenesis and shows NFIA's distinct presence in neural progenitor domains for motor neurons of the spinal cord (Deneen et al., 2006; Glasgow et al., 2017). NFIA expression in the developing spinal cord is regulated through the dynamic complex of motor neuron genes that aid in development, ISL1 and LHX3 (Glasgow et al., 2017). Furthermore, regulation of NFIA expression is differentially regulated in spinal cord populations where lineage specific chromatin loops determine whether or not NFIA is expressed in glial cell precursors or motor neuron precursors, but its unique role in the motor neuron loop has not been thoroughly defined (Glasgow et al., 2017). Given NFIA's role as a transcriptional regulator and its expression in developing MNs, our study aimed to define the function of NFIA in spinal motor neurons. To do this, we used RCAS NFIA and RCAS NFIAi electroporation to overexpress and knockdown NFIA, respectively, in chicken spinal cords. We also developed two transgenic mouse lines where NFIA was conditionally deleted in HB9 MNs and ISL1MNs creating $NFIA^{FF}$;HB9-CRE mice and $NFIA^{FF}$;ISL1-CRE, respectively. The expression of NFIA was analyzed with fellow motor neuron markers ISL1, ISL2, HB9/MNR2, FOXP1, LHX3, and LIM1/2, ventral markers CHX10 and FOXP2, and dorsal marker PAX2.

Significance of Findings

Overexpression of NFIA via RCAS NFIA electroporation did not lead to any significant findings, suggesting NFIA is not sufficient to induce any changes in MN pools of the spinal cord. In our mutant mouse models, we also found no change in the motor neuron specification or

organization at thoracic levels of the spinal cord. However, changes in MN populations and column organization were observed at the brachial/lumbar regions of the spinal cord. Our phenotypes were not expressed until E13.5, signifying the loss of NFIA has an impact after the specification of MNs. NFIA is not required for the formation of MNs in the developing spinal cord.

In both chicken (RCAS-NFIAi) and mouse models, reduction and migration of LIM1/2 was observed. LIM1/2 cells migrate from LMC-l to LMC-m MNs. In the chicken, only reduction of FOXP1 was found but in our mouse models, we saw both reduction of FOXP1 cells in LMC-m/l MNs and increased migration of FOXP1 from the MN pools out to the ventral and dorsal regions of the spinal cord. Additionally, we found reduced expression and migration of FOXP2 from ventral pools of the spinal cord in both transgenic mouse lines. We also observed reduced PAX2 expression in dorsal pools of the spinal cord, but only in $NFIA^{FF}$;ISL1-CRE spinal cords.

Future Directions

The findings of this thesis advise many exciting future studies. To begin, the loss of NFIA has clear effects on LIM1/2 and FOXP1, across all models, and suggests that NFIA is necessary for the organization of MNs in the LMC MN pools. Future research should consider examining LMC MNs more closely to see if there are deficits with axonal targeting to the limbs, motor output, or motor control over the limbs. Behavioral observation of mice at different stages could give better insight into the effects of disorganization within LMC MNs. This would allow us to see how the deletion of NFIA impacts motor ability directly. From six weeks on to one year of life, hanging tests, pain tests, whisker response, and analysis of general health and aggression could be evaluated to give insight into coordination, motor abilities, pain reflexes, and more in our transgenic mice.

Initial, basic neuroscreens in our lab suggest that transgenic mice have decreased reflex responses to pain, but this hypothesis needs to be verified with more complex behavioral analysis and more mice.

Furthermore, past research on FOXP1 reveals this transcription factor to be critical for cell expression patterns in the PGC and LMC MNs and axonal guidance and innervation from the LMCs to limbs and the loss of FOXP1 has been linked to severe neurodegenerative disorders, like Huntington's Disorder (Rousso et al., 2008; Titus et al., 2012; Adams et al., 2015). The next step from this study would be to ask whether or not the reduction and migration we see from FOXP1 is leading to more severe nerve and motor damage. Moreover, biochemical assays and RNA sequencing experiments to profile the brachial/thoracic spinal cord after E13.5 could give us better insight into what is happening genomically and transcriptionally with respect to FOXP1, LIM1/2, and their interactions with NFIA.

Interestingly, past research has shown that alteration of gene expression in HB9 cells of spinal motor neurons had serious implications. Mice with an HB9 mutation experienced weight loss as adults, decreased motor ability, and curving as the spine (Gogliotti et al., 2012). Since we alter the expression of NFIA in HB9 MNs, there is reason to ask if the mouse models used in this research could lead to similar results. Finally, a 2019 single cell profiling of the developmental mouse brain shows NFIA is mainly present in lower gamma motor neurons of the spinal cord. Cell expression in these gamma motor neurons emerges after embryonic development (Rosenberg et al., 2019); therefore, going forward, an area of research could be assessing the role of NFIA in adult MNS. Initial studies could evaluate the co-expression of NFIA with gamma motor neuron markers KCNA5 or ESRRB in early post-natal stages through adulthood of wildtype mice. Then,

an NFIA conditional knockout mouse in adult MNs could be used to see how these gamma motor neuron gene expressions and spinal cords are altered.

Another study would be to analyze NFIA and its impact in more transgenic mouse lines. Our $NFIA^{FF}$;ISL1-CRE mouse line demonstrates a significant impact on dorsal marker PAX2, suggesting we need to conduct more analysis of dorsal markers. We are currently breeding a NESTIN-CRE mouse line in order to knockout NFIA completely. In addition, we could analyze conditional deletion of NFIA in dorsal populations using a PAX3-CRE mouse line to decouple the dorsal and ventral NFIA phenotypes. With a diverse set of transgenic mice, we can begin to make patterns and draw trends around NFIA's exact role in the spinal cord.

Lastly, our motor neuron culture system can lead to some exciting new studies. The establishment of a motor neuron culture provides us flexibility and allows us to do electrophysiological experiments, like patch-clamping the neurons in order to study their ionic properties. In the future, we can use the culture to compare our transgenic mouse to control models, enabling us to exam the polarity, shape, and size of our mutated motor neurons. We are also working on developing a neonatal culture, in order to analyze motor neurons between p1-p3, and an adult culture to analyze mice over six weeks old.

Ultimately, in this study, we illustrate that NFIA is a prominent transcription factor of developmental motor neurons. The loss of NFIA does indeed have a causal effect in motor neuron columns. Hopefully, this study can begin to answer larger questions about the role of NFIA in the motor neuron chromatin loop of the spinal cord. Future research can take this steppingstone and ask questions that go beyond development.

FIGURES

FIGURE 1. Motor Neuron Column Organization in Embryonic Chick Spinal Cord Shows NFIA in MMC, LMC-m, and LMC-l MNs. Chicken spinal cords were harvested at gestational day E5. The spinal cords were fixed and embedded in OCT and sectioned via cryostat at 20 micrometers onto glass slides. These sections were immunostained for various MN markers, imaged with IHC fluorescence microscopy, and cells were counted. White line = scale bar; 100 um. (A) FOXP1 and MNR2 expression and summary of how these markers organize in the LMC-l, LMC-m, and MMC columns of the spinal cord. (B) ISL 1 and LIM1/2 expression and summary of organization in MNs (C) FOXP1 and ISL2 expression and summary of organization in MNs (D) ISL 1 and LHX3 expression and summary of of organization in MNs (E) NFIA and MNR2 expression and summary of organization in MNs, showing NFIA in every MN column of this level.

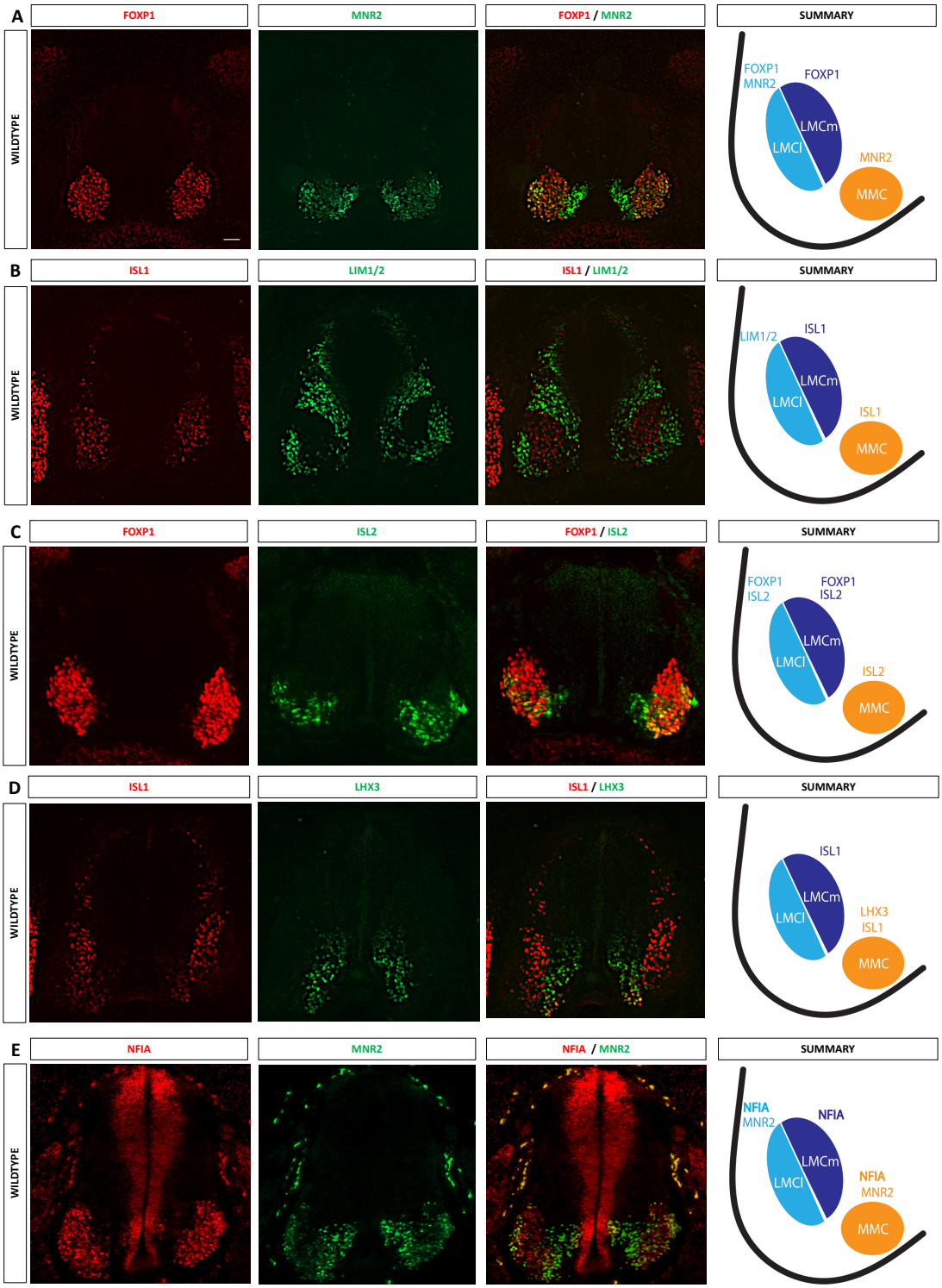
A
FOXP1
MNR2
FOXP1 / MNR2
SUMMARY
WILDTYPE
FOXP1
MNR2
FOXP1
LMCm
LMCl
MNR2
MMC
B
ISL1
LIM1/2
ISL1 / LIM1/2
SUMMARY
WILDTYPE
LIM1/2
ISL1
LMCm
LMCl
ISL1
MMC
C
FOXP1
ISL2
FOXP1 / ISL2
SUMMARY
WILDTYPE
FOXP1
ISL2
FOXP1
ISL2
LMCm
LMCl
ISL2
MMC
D
ISL1
LHX3
ISL1 / LHX3
SUMMARY
WILDTYPE
ISL1
LMCm
LMCl
LHX3
ISL1
MMC
E
NFIA
MNR2
NFIA / MNR2
SUMMARY
WILDTYPE
NFIA
MNR2
NFIA
LMCm
LMCl
NFIA
MNR2
MMC

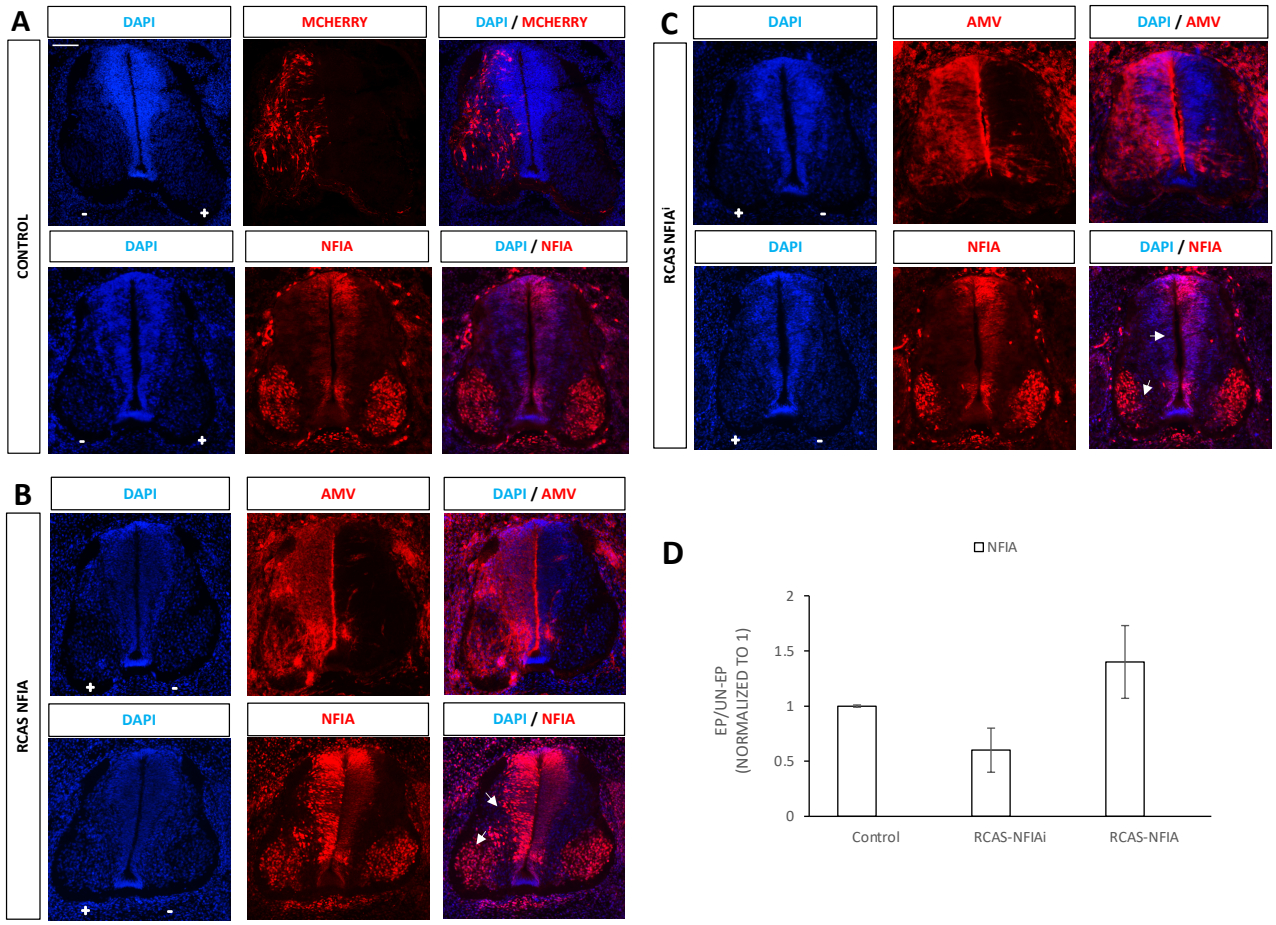

FIGURE 2. NFIA is Overexpressed in RCAS NFIA Spinal Cords and Knocked Down in RCAS NFIAi Spinal Cords. Chicken spinal cords were harvested on E5. The spinal cords were fixed and embedded in OCT and sectioned via cryostat at 20 micrometers onto glass slides. These sections were immunostained for NFIA and AMV presence, imaged with IHC fluorescence microscopy and mCHERRY, and cells were counted. White line = scale bar; 100 um. (A) mCHERRY and NFIA IHC in RCAS control spinal cords. (B) AMV and NFIA IHC in RCAS NFIA overexpression model. (C) AMV and NFIA IHC in RCAS NFIAi knockdown model. (D) Cell counts of NFIA of the wildtype and mutant spinal cords

FIGURE 3. Altered Expression of LIM1/2 and FOXP1 in NFIAi Spinal Cords. Chicken spinal cords electroporated with RCAS-NFIAi were harvested on E5. The spinal cords were fixed and embedded in OCT and sectioned via cryostat at 20 micrometers onto glass slides. These sections were immunostained for ISL1, LIM1/2, FOXP1, and ISL2, imaged with IHC fluorescence microscopy, and cells were counted. (A) ISL1 and LIM1/2 expression in control and RCAS NFIAi spinal cords. White line = scale bar; 100 um. (B) Summary of LIM1/2 migration phenotype in RCAS NFIA spinal cords. (C) FOXP1and ISL2 expression in control and RCAS NFIAi spinal cords. (D) Summary of FOXP1 reduction phenotype in RCAS NFIA spinal cords. (E) Cell analysis of (A) demonstrating reduction of LIM1/2 and increase in overlapping cells. (F) Cell analysis of (C) demonstrating reduction of FOXP1 and increase in overlapping cells. (G) Caspase3 IHC of control vs RCAS NFIAi spinal cords. (H). Cell analysis of Caspase3 IHC (G), demonstrating no significant difference.

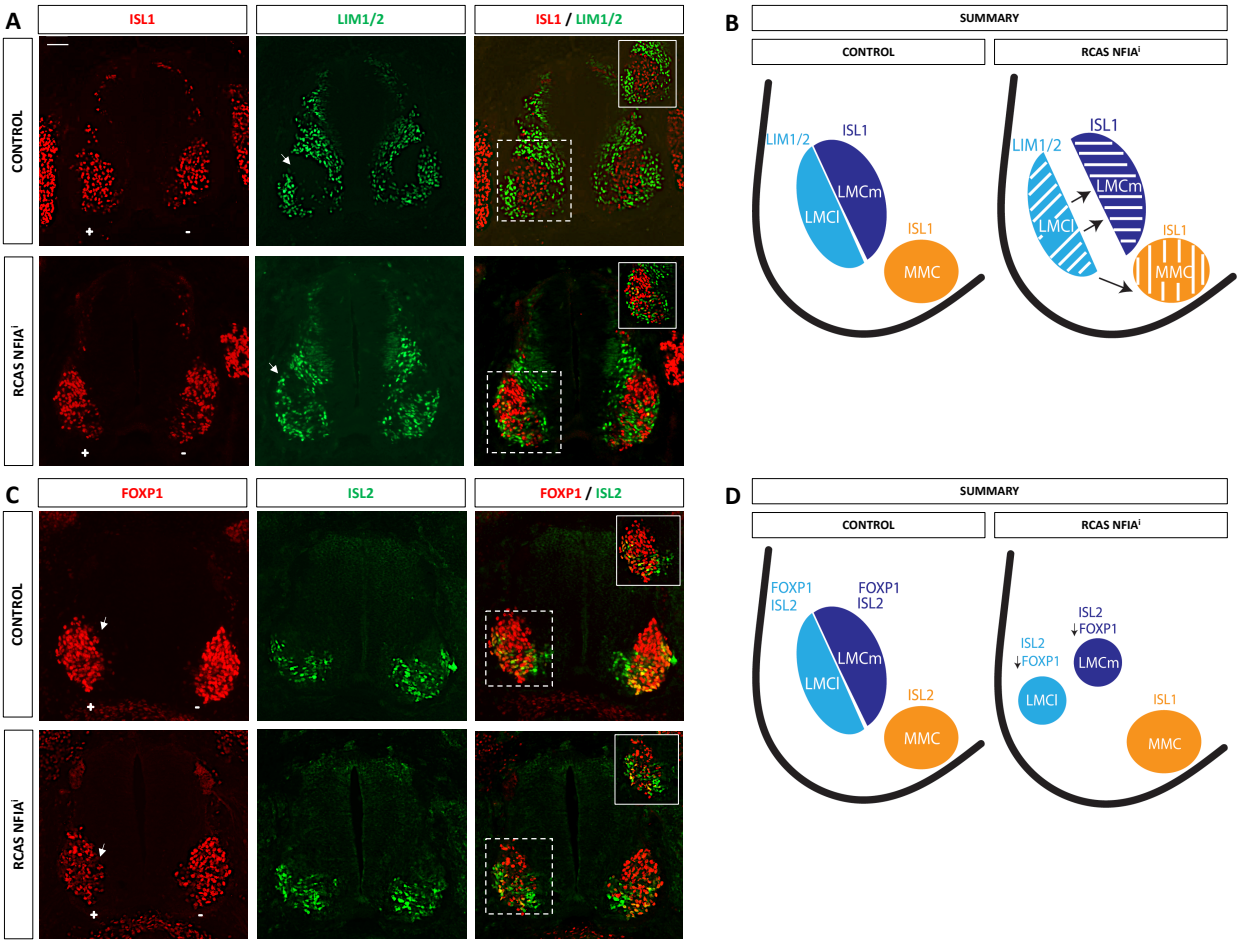
A
ISL1
LIM1/2
ISL1 / LIM1/2
CONTROL
RCAS NFIA^I
B
SUMMARY
CONTROL
RCAS NFIA^I
LIM1/2
ISL1
LMCm
LMCl
MMC
C
FOXP1
ISL2
FOXP1 / ISL2
D
FOXP1
ISL2
↓FOXP1

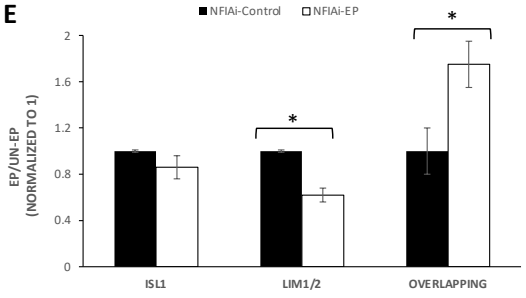
E
NFIAi-Control
NFIAi-EP
EP/UN-EP (NORMALIZED TO 1)
ISL1
LIM1/2
OVERLAPPING

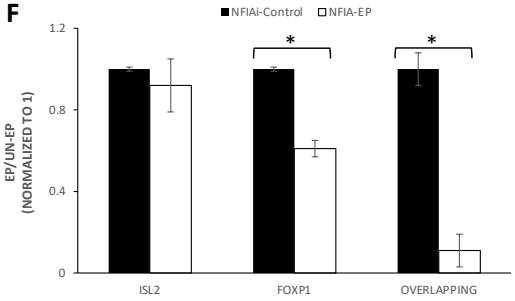
F
NFIAi-Control
NFIA-EP
EP/UN-EP (NORMALIZED TO 1)
ISL2
FOXP1
OVERLAPPING

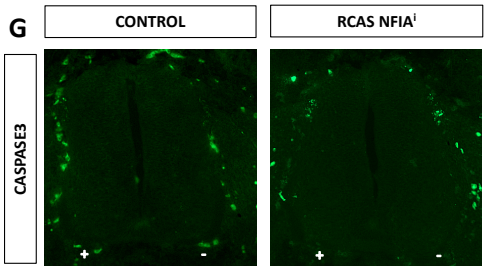
G
CONTROL
RCAS NFIA^I
CASPASE3

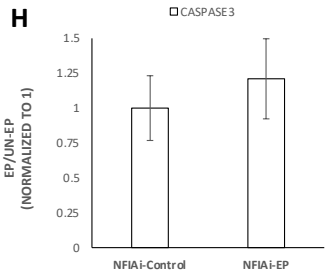
H
CASPASE3
EP/UN-EP (NORMALIZED TO 1)
NFIAi-Control
NFIAi-EP

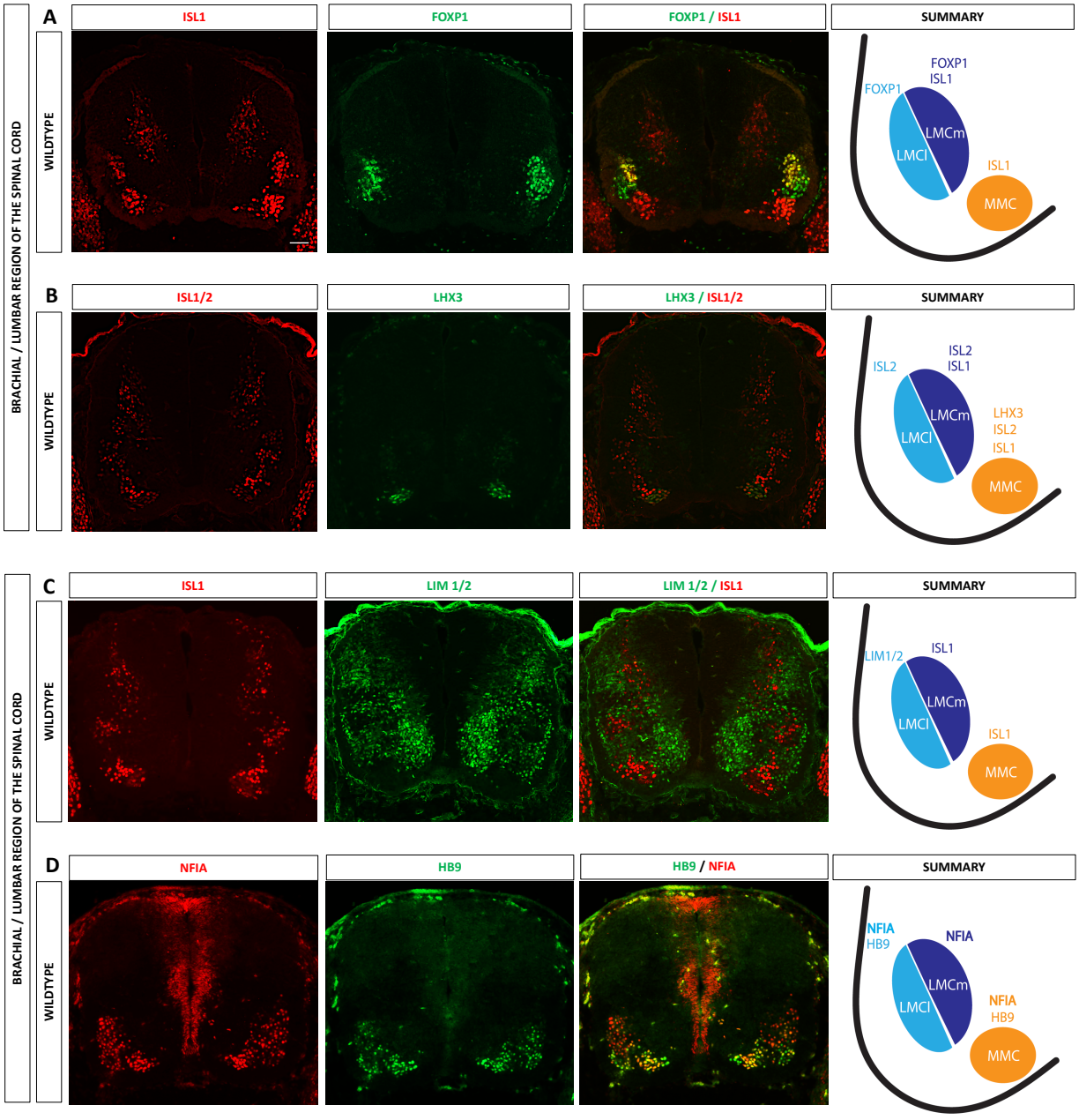

FIGURE 4: Motor Neuron Column Organization in Embryonic Chick Spinal Cord Shows NFIA in MMC, LMC-m, LMC-l, and HMC MNs. Mouse spinal cords were harvested on E5. The spinal cords were fixed and embedded in OCT and sectioned via cryostat at 20 micrometers onto glass slides. These sections were immunostained for various MN markers at the brachial/lumbar and thoracic levels of the spinal cord and imaged with IHC fluorescence microscopy. White line = scale bar; 100 um. (A-D) ISL1 and FOXP1, ISL1/2 and LHX3, ISL1 and LIM1/2, and NFIA and HB9 expression in the Brachial/Lumbar region of the spinal cord. To the right of each IHC combination is a summary of how these markers organize in the LMC-l, LMC-m, and MMC columns of the SC.

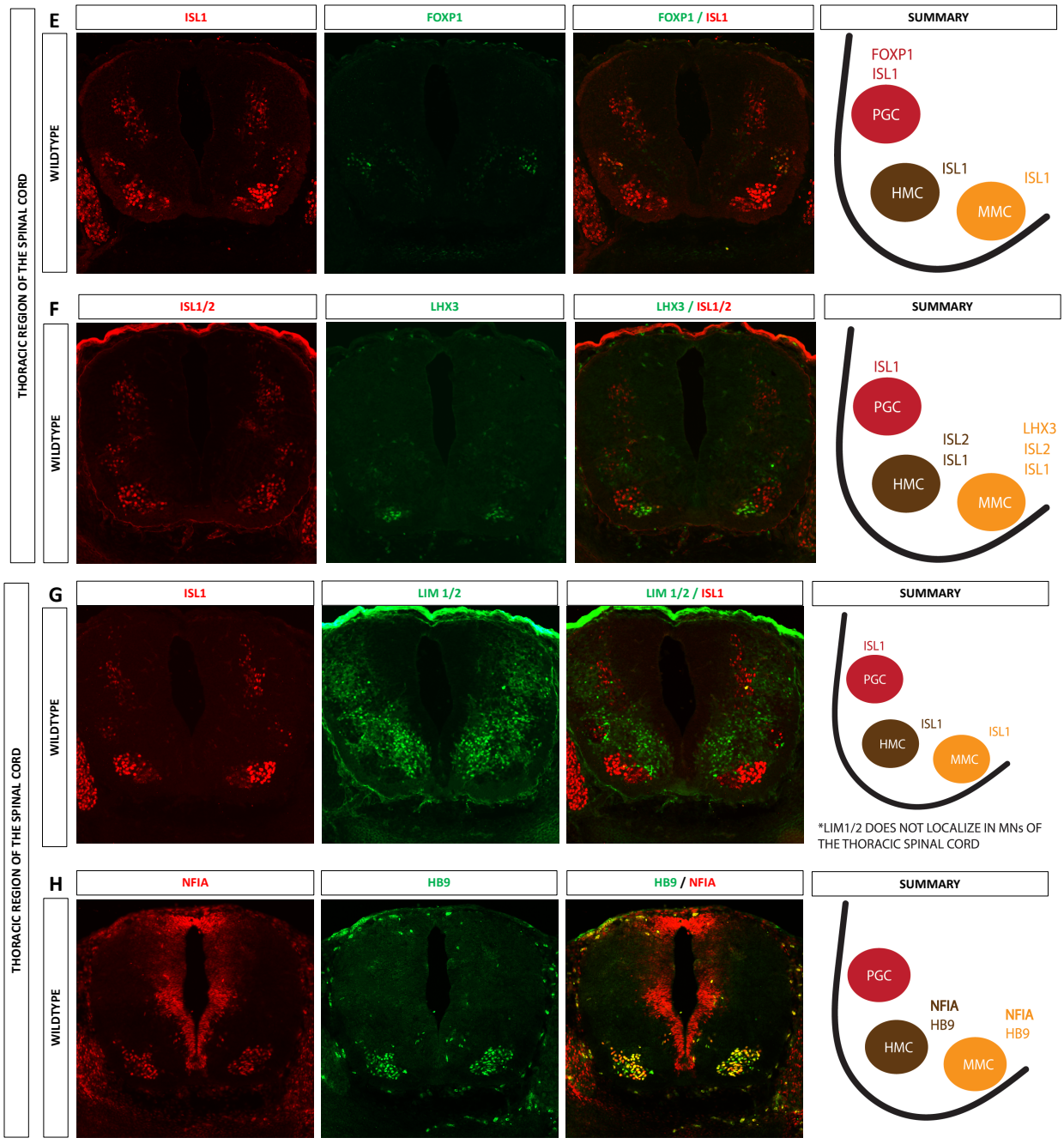

FIGURE 4: Motor Neuron Column Organization in Embryonic Chick Spinal Cord Shows NFIA in MMC, LMC-m, LMC-l, and HMC MNs (continued). (E-F) ISL1 and FOXP1, ISL1/2 and LHX3, ISL1 and LIM1/2, and NFIA and HB9 expression in the Thoracic region of the spinal cord. To the right of each IHC combination is a summary of how these markers organize in the PGC, HMC, and MMC columns of the SC. NFIA is expressed in MMC, LMC-m, LMC-l, and HMC MNs.

FIGURE 5: Conditional Deletion of NFIA in HB9 CRE Neurons Leads to Reduced Expression and Migration of LIM1/2 and FOXP1. Mouse spinal cords were harvested on E13.5, 16.5, and 18.5. The spinal cords were fixed and embedded in OCT and sectioned via cryostat at 20 micrometers onto glass slides. These sections were immunostained at the brachial/lumbar levels of the spinal cord and imaged with IHC fluorescence microscopy. White line = scale bar; 100 um. (A) Schematic of our HB9 CRE TD Tomato system. (B) IHC of TD Tomato in $NFIA^{F/F}$;HB9 CRE TD Tomato E12.5 spinal cord. (C) NFIA and HB9 IHC in control and $NFIA^{F/F}$;HB9 CRE in E12.5 spinal cords. (D). Cell analysis of NFIA and HB9 IHC in C. (E-F) ISL1 and LIM1/2 IHC in control and $NFIA^{F/F}$;HB9 CRE in E13.5 spinal cords and corresponding summaries. (G-H) ISL1 and FOXP1 IHC in control and $NFIA^{F/F}$;HB9 CRE in E13.5 spinal cords and corresponding summaries. (I) Cell analysis of E-F demonstrating decreased expression of LIM1/2 and reduced overlapping cells between ISL1 and LIM1/2. (J-K) Cell analysis of G-H demonstrating decreased expression of FOXP1 in MNs, reduced overlapping cells between ISL1 and LIM1/2, and increased migration of FOXP1 cells out of MN pools (L-M) Caspase3 IHC in control and $NFIA^{F/F}$;HB9 CRE in E13.5 spinal cords and the cell analysis, demonstrating no significant increase in cell death of knockdown model. (N-O) FOXP1 IHC in control and $NFIA^{F/F}$;HB9 CRE in E13.5, 16.5, and 18.5 spinal cords.

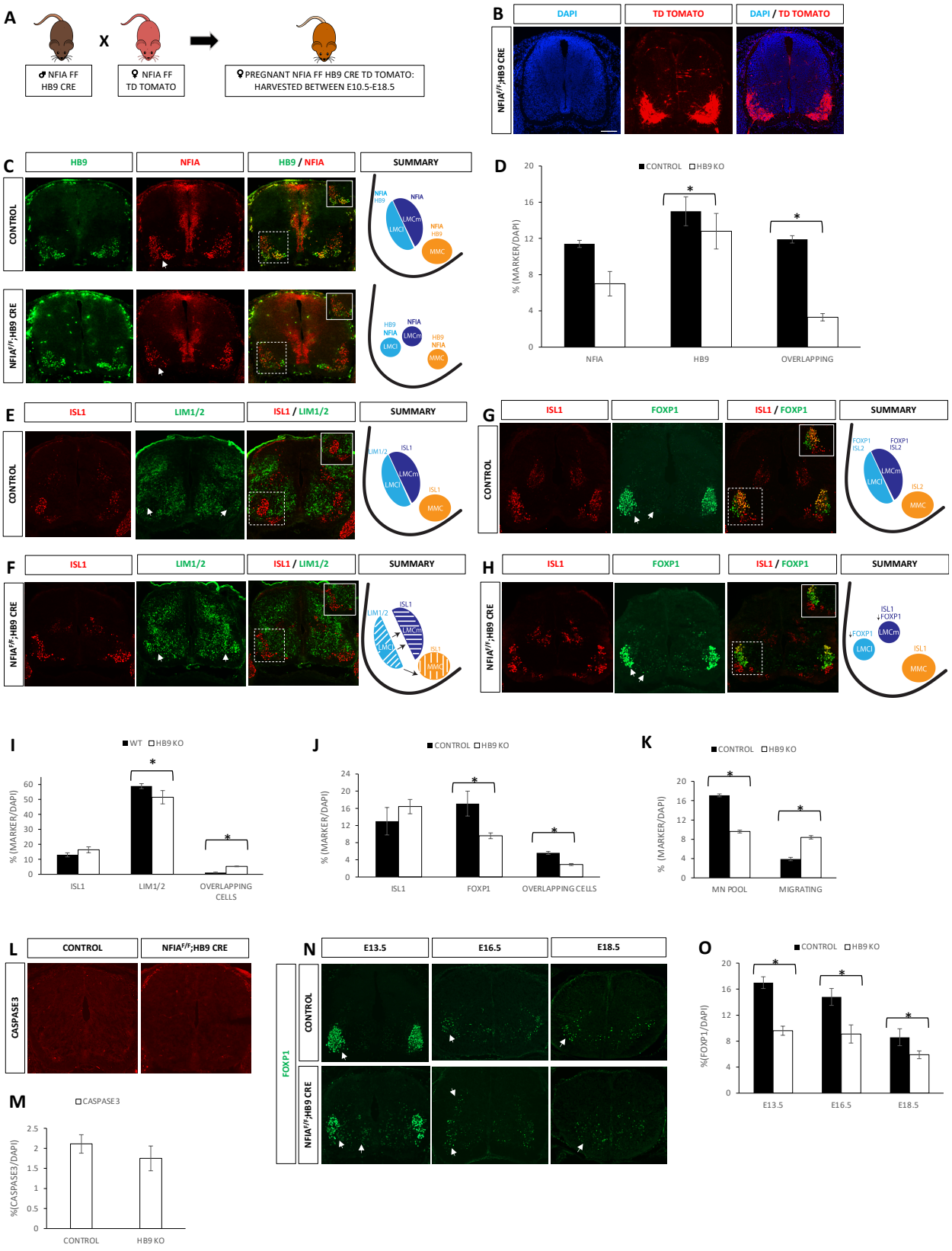
A
♂ NFIA FF HB9 CRE
X
♀ NFIA FF TD TOMATO
♀PREGNANT NFIA FF HB9 CRE TD TOMATO: HARVESTED BETWEEN E10.5-E18.5
B
DAPI
TD TOMATO
DAPI / TD TOMATO
NFIA F/F;HB9 CRE
C
HB9
NFIA
HB9 / NFIA
SUMMARY
CONTROL
NFIA F/F;HB9 CRE
D
CONTROL
HB9 KO
% (MARKER/DAPI)
NFIA
HB9
OVERLAPPING
E
ISL1
LIM1/2
ISL1 / LIM1/2
SUMMARY
CONTROL
F
NFIA F/F;HB9 CRE
G
ISL1
FOXP1
ISL1 / FOXP1
SUMMARY
CONTROL
H
NFIA F/F;HB9 CRE
I
WT
HB9 KO
% (MARKER/DAPI)
ISL1
LIM1/2
OVERLAPPING CELLS
J
CONTROL
HB9 KO
% (MARKER/DAPI)
ISL1
FOXP1
OVERLAPPING CELLS
K
CONTROL
HB9 KO
% (MARKER/DAPI)
MN POOL
MIGRATING
L
CONTROL
NFIA F/F;HB9 CRE
CASPASE3
M
CASPASE3
%(CASPASE3/DAPI)
CONTROL
HB9 KO
N
E13.5
E16.5
E18.5
FOXP1
CONTROL
NFIA F/F;HB9 CRE
O
CONTROL
HB9 KO
%(FOXP1/DAPI)
E13.5
E16.5
E18.5

FIGURE 6: Conditional Deletion of NFIA in ISL1 CRE Neurons Leads to Reduced Expression and Migration of LIM1/2 and FOXP1. Mouse spinal cords were harvested on E13.5, 16.5, and 18.5. The spinal cords were fixed and embedded in OCT and sectioned via cryostat at 20 micrometers onto glass slides. These sections were immunostained at the brachial/lumbar levels of the spinal cord and imaged with IHC fluorescence microscopy. White line = scale bar; 100 um. (A) Schematic of our ISL1 CRE TD Tomato system. (B) IHC of TD Tomato in $NFIA^{F/F}$;ISL1 CRE TDTOMATO E12.5 spinal cord. (C) NFIA and ISL1 IHC in control and $NFIA^{F/F}$;ISL1 CRE in E12.5 spinal cords. (D). Cell analysis of NFIA and HB9 IHC in C, demonstrating completely knockout of NFIA. (E-F) ISL1 and LIM1/2 IHC in control and $NFIA^{F/F}$;ISL1 CRE in E13.5 spinal cords and corresponding summaries. (G-H) ISL1 and FOXP1 IHC in control and $NFIA^{F/F}$;ISL1 CRE in E13.5 spinal cords and corresponding summaries. (I) Cell analysis of E-F demonstrating decreased expression of LIM1/2 and reduced overlapping cells between ISL1 and LIM1/2. (J-K) Cell analysis of G-H demonstrating decreased expression of FOXP1 in MNs, reduced overlapping cells between ISL1 and LIM1/2, and increased migration of FOXP1 cells out of MN pools (L-M) Caspase3 IHC in control and $NFIA^{F/F}$;ISL1 CRE in E13.5 spinal cords and the cell analysis, demonstrating no significant increase in cell death of knockdown model. (N-O) FOXP1 IHC in control and $NFIA^{F/F}$;ISL1 CRE in E13.5, 16.5, and 18.5 spinal cords.

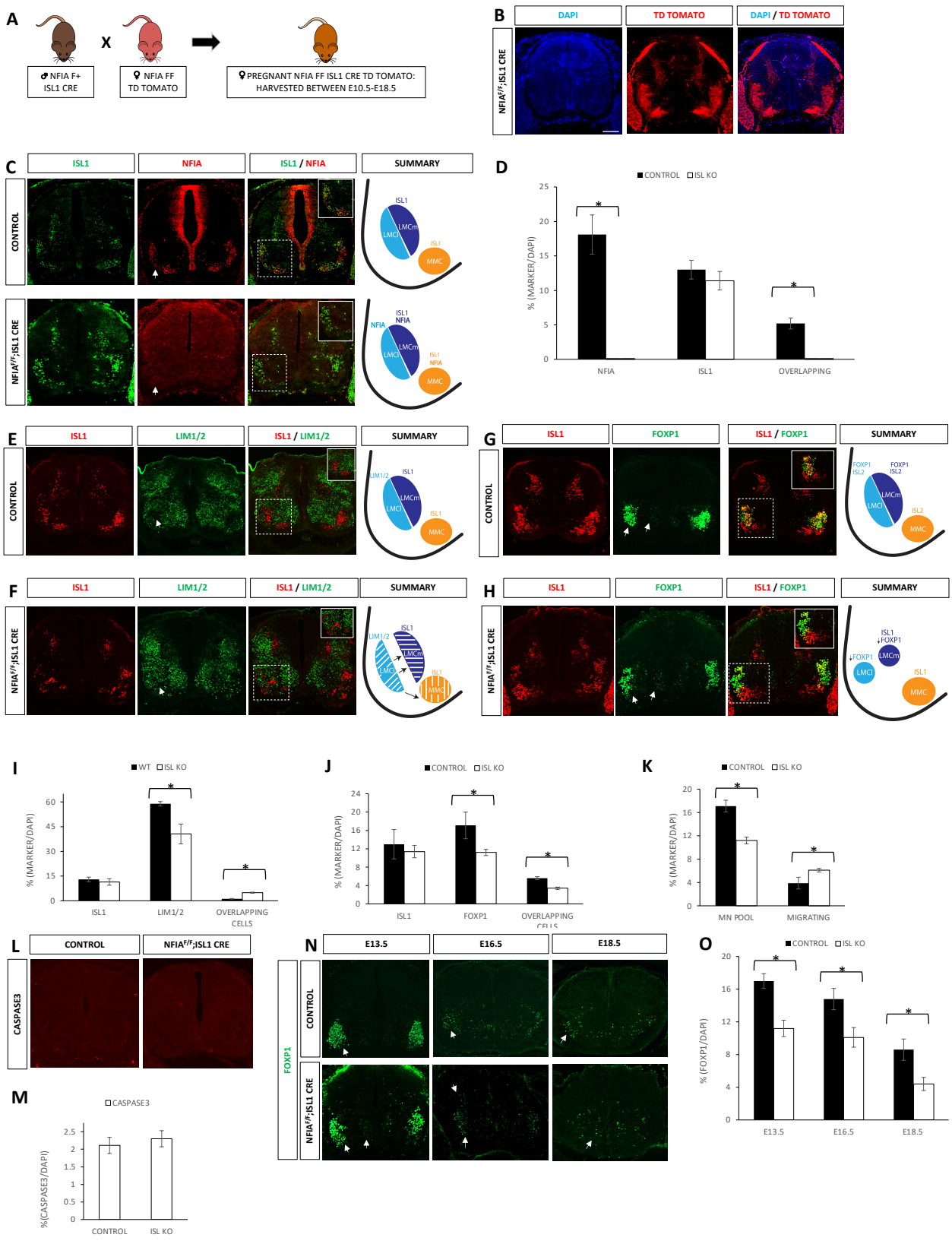
A
♂ NFIA F+
ISL1 CRE
X
♀ NFIA FF
TD TOMATO
♀ PREGNANT NFIA FF ISL1 CRE TD TOMATO:
HARVESTED BETWEEN E10.5-E18.5
B
DAPI
TD TOMATO
DAPI / TD TOMATO
NFIA F/F;ISL1 CRE
C
ISL1
NFIA
ISL1 / NFIA
SUMMARY
CONTROL
NFIA F/F;ISL1 CRE
LMCm
LMCl
MMC
D
CONTROL
ISL KO
% (MARKER/DAPI)
NFIA
ISL1
OVERLAPPING
E
ISL1
LIM1/2
ISL1 / LIM1/2
SUMMARY
CONTROL
F
NFIA F/F;ISL1 CRE
G
ISL1
FOXP1
ISL1 / FOXP1
SUMMARY
CONTROL
H
NFIA F/F;ISL1 CRE
I
WT
ISL KO
% (MARKER/DAPI)
ISL1
LIM1/2
OVERLAPPING CELLS
J
CONTROL
ISL KO
% (MARKER/DAPI)
ISL1
FOXP1
OVERLAPPING CELLS
K
CONTROL
ISL KO
% (MARKER/DAPI)
MN POOL
MIGRATING
L
CONTROL
NFIA F/F;ISL1 CRE
CASPASE3
M
CASPASE3
%(CASPASE3/DAPI)
CONTROL
ISL KO
N
E13.5
E16.5
E18.5
FOXP1
CONTROL
NFIA F/F;ISL1 CRE
O
CONTROL
ISL KO
% (FOXP1/DAPI)
E13.5
E16.5
E18.5

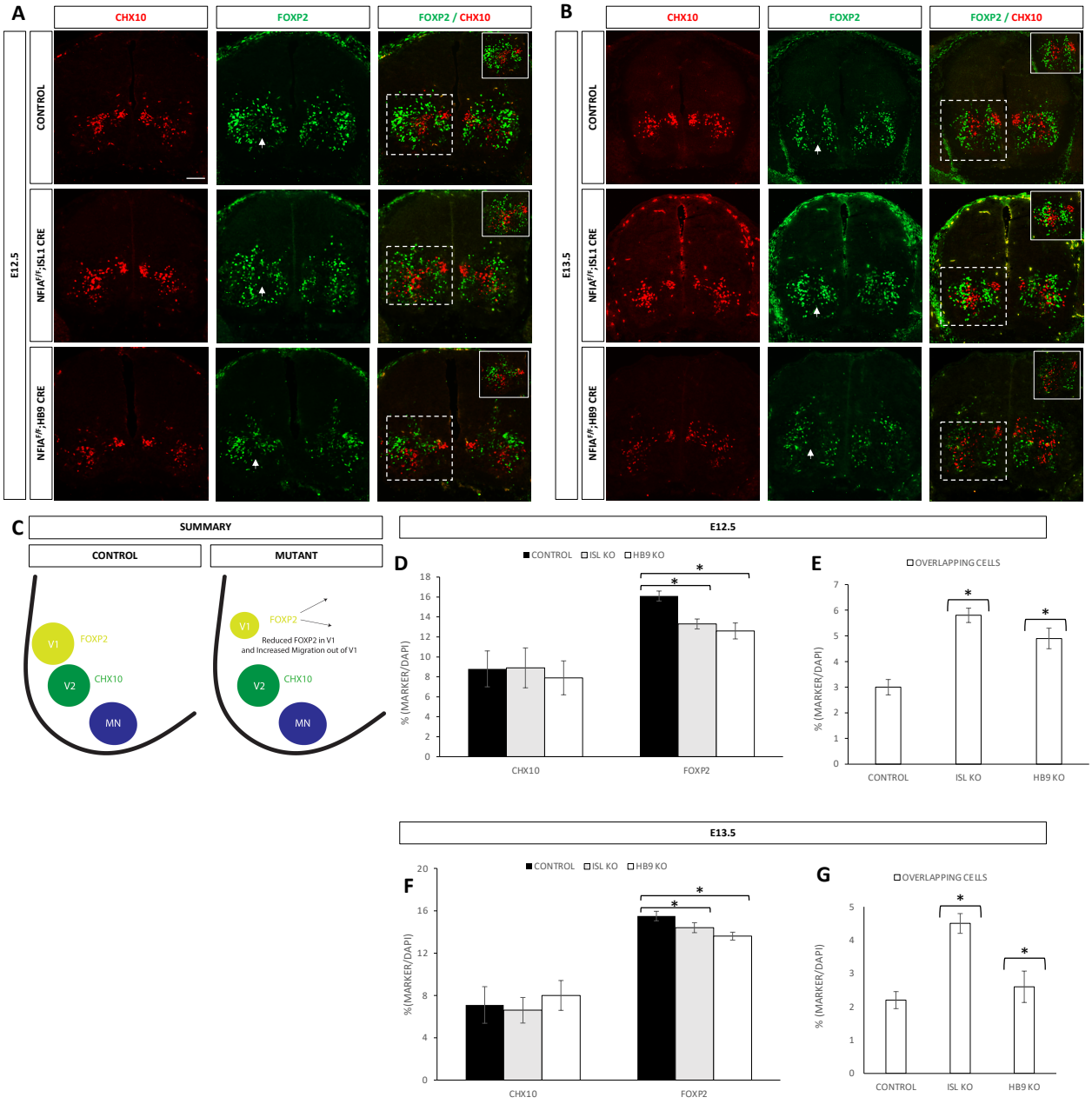

FIGURE 7: Reduction and Migration of FOXP2 in HB9 and ISL1 Transgenic Spinal Cords. Embryonic mouse spinal cords were harvested on E12.5 and E13.5. The spinal cords were fixed and embedded in OCT and sectioned via cryostat at 20 micrometers onto glass slides. The brachial/lumbar regions of the spinal cord were immunostained for CHX10 and FOXP2, imaged with IHC fluorescence microscopy, and cells were counted. White line = scale bar; 100 um. (A) CHX10 and FOXP2 IHC expression in the E12.5 wildtype and mutant spinal cords. (B) CHX10 and FOXP2 IHC expression in E13.5 wildtype and mutant spinal cords. (C) Summary of FOXP2 phenotype. (D-E) Cell analysis of CHX10 and FOXP1 E12.5 spinal cords, demonstrating reduction of FOXP2 and increased overlapping cell expression between CHX10 and FOXP2. (F-G) Cell analysis of CHX10 and FOXP1 E13.5 spinal cords, demonstrating reduction of FOXP2 and increased overlapping cell expression between CHX10 and FOXP2.

FIGURE 8: Reduction of PAX2 in NFIA$^{F/F}$;ISL1 CRE Spinal Cords. Embryonic mouse spinal cords were harvested on E12.5 and E13.5. Spinal cords were fixed and embedded in OCT and sectioned via cryostat at 20 micrometers onto glass slides. The brachial/lumbar regions of the spinal cord were immunostained for PAX2 and LIM1/2, imaged with IHC fluorescence microscopy, and cells were counted. White line = scale bar; 100 um. (A) PAX2 and LIM1/2 IHC expression in the E12.5 wildtype and mutant spinal cords. (B) PAX2 and LIM1/2 IHC expression in E13.5 wildtype and mutant spinal cords. LIM1/2 arrow heads point to the reduction of LIM1/2 cells in dorsal regions (C) Summary of PAX2 and LIM1/2 phenotype. (D-E) Cell analysis of PAX2 and LIM1/2 E12.5 spinal cords, demonstrating reduction of PAX2 and decreased overlapping cell expression between PAX2 and LIM1/2 in ISL1 transgenic mice. (F-G) Cell analysis of PAX2 and LIM1/2 E13.5 spinal cords, demonstrating reduction of PAX2 and decreased overlapping cell expression between PAX2 and LIM1/2, again in only NFIA$^{F/F}$;ISL1 CRE mice.

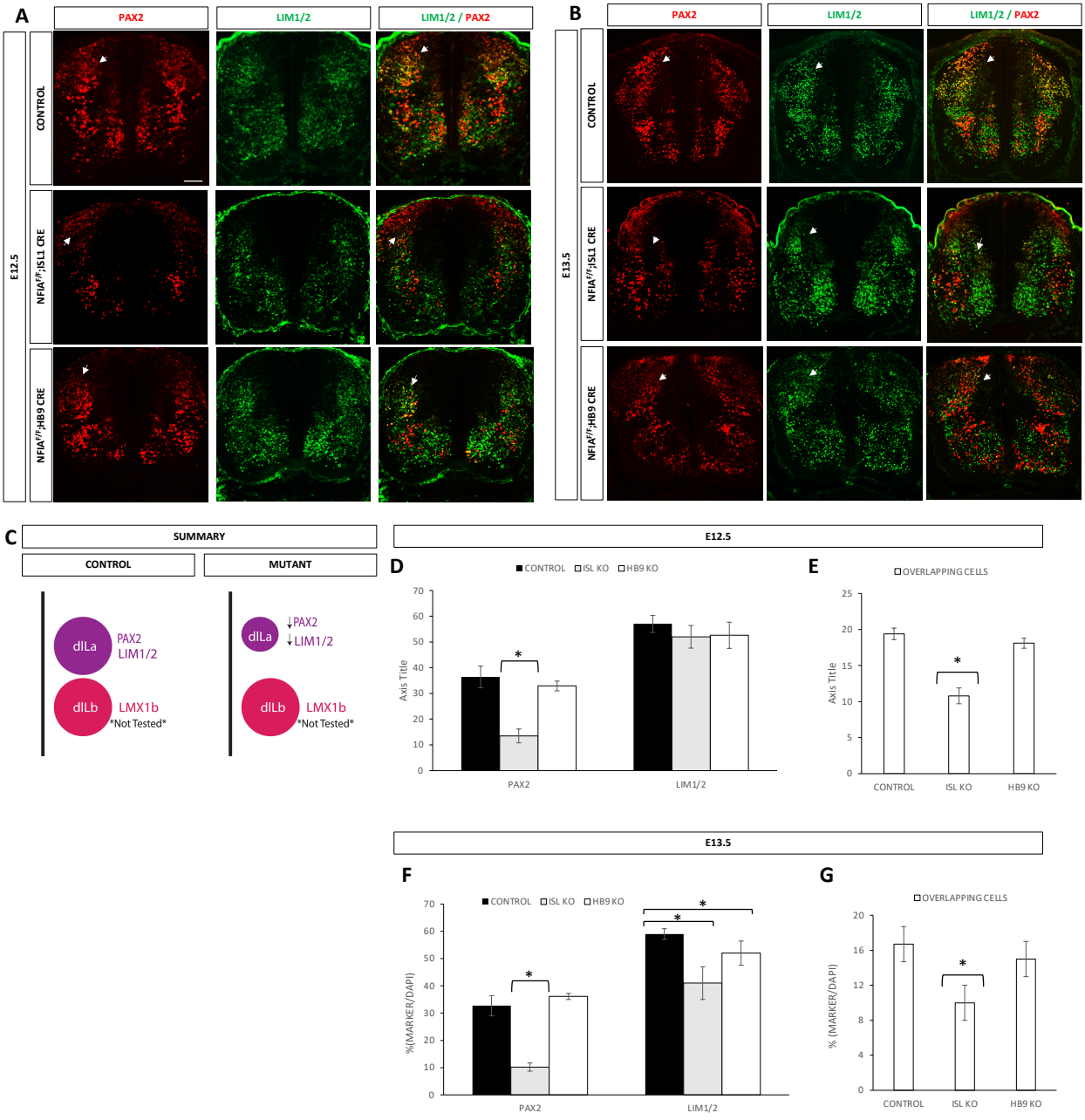
A
PAX2
LIM1/2
LIM1/2 / PAX2
E12.5
CONTROL
NFIA F/F;ISL1 CRE
NFIA F/F;HB9 CRE
B
PAX2
LIM1/2
LIM1/2 / PAX2
E13.5
CONTROL
NFIA F/F;ISL1 CRE
NFIA F/F;HB9 CRE
C
SUMMARY
CONTROL
MUTANT
dILa
PAX2
LIM1/2
dILb
LMX1b
Not Tested
dILa
↓PAX2
↓LIM1/2
dILb
LMX1b
Not Tested
E12.5
D
CONTROL ISL KO HB9 KO
Axis Title
PAX2
LIM1/2
E
OVERLAPPING CELLS
Axis Title
CONTROL
ISL KO
HB9 KO
E13.5
F
CONTROL ISL KO HB9 KO
%(MARKER/DAPI)
PAX2
LIM1/2
G
OVERLAPPING CELLS
% (MARKER/DAPI)
CONTROL
ISL KO
HB9 KO

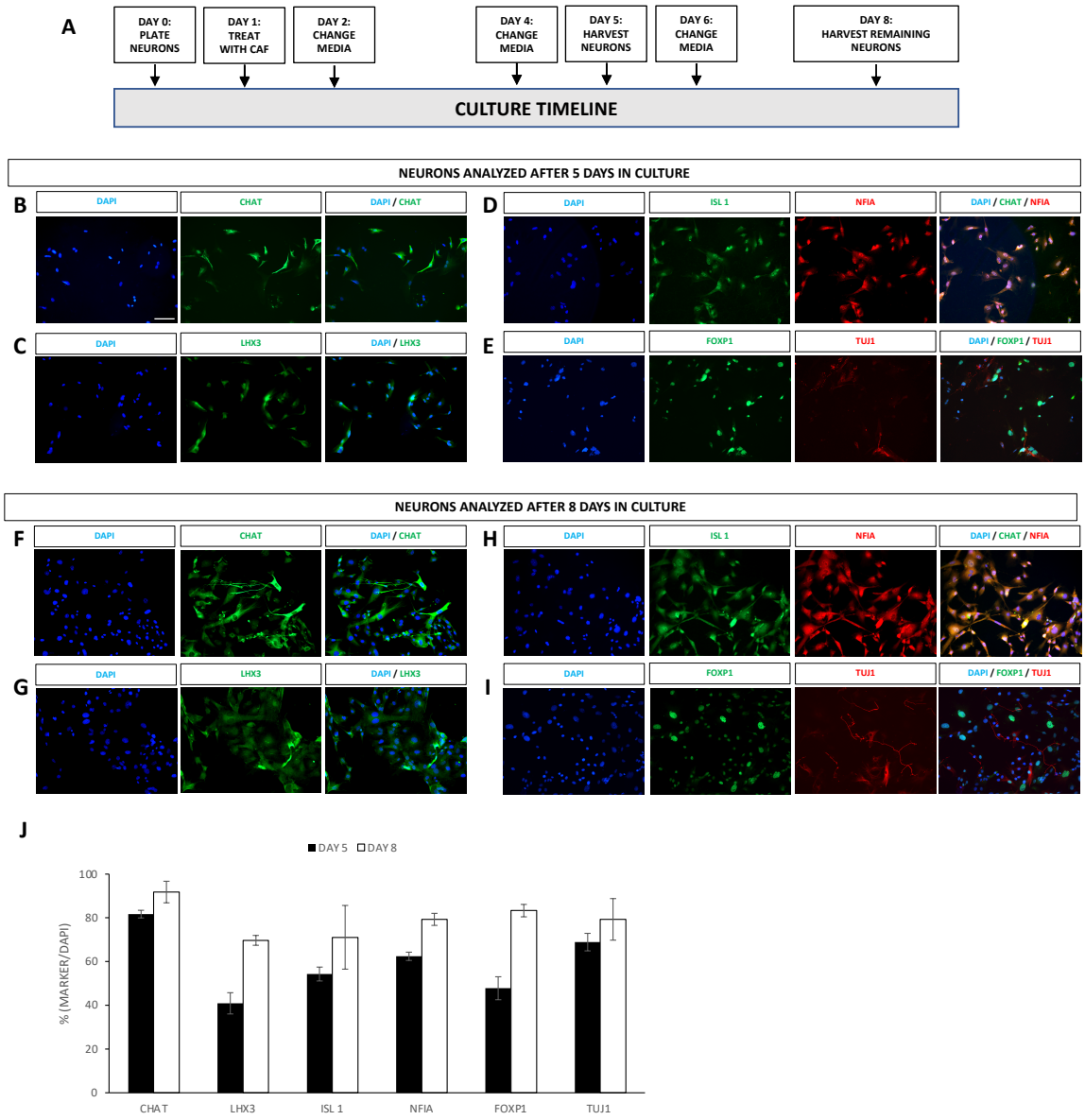

FIGURE 9: Wildtype Embryonic Motor Neurons Analyzed in Cell Culture. Spinal cords harvested at e14.5 provided motor neurons for a cell culture technique. Cells were collected from 14 embryonic spinal cords and plated at 150,000 cells/well of a 24 well plate. White line = scale bar; 50 um. (A) Protocol/Cell Culture technique (B-E): Immunostaining of motor neuron markers CHAT, LHX3, NFIA, ISL1, FOXP1, and TUJ1 5 days after cells were plated. (F-I) Immunostaining of CHAT, LHX3, NFIA, ISL1, FOXP1, and TUJ1 8 days after cells were plated. (J) Counts of motor neuron markers analyzed in days 5 and 8 immunostainings.

REFERENCES

1. Abbas, Tarek & Dutta, Anindya. (2009). Abbas T, Dutta Ap21 in cancer: intricate networks and multiple activities. Nat Rev Cancer 9: 400-414. Nature reviews. Cancer. 9. 400-14.

2. Adams KL, Rousso DL, Umbach JA, Novitch BG. Foxp1-mediated programming of limb-innervating motor neurons from mouse and human embryonic stem cells. Nat Commun. 2015 Apr 14;6:6778.

3. Alaynick, W., Jessell, T.W., Plaff, S. L., 2011. Snapshot: spinal cord development. Cell. 146, 178-178.e1

4. Arabsolghar, Rita & Rasti, Mozhgan. (2012). Optimal Electroporation Condition for Small Interfering RNA Transfection into MDA-MB-468 Cell Line. Iranian journal of medical sciences. 37. 187-93.

5. Arber, Silvia. (2008). FoxP1: Conducting the Hox symphony in spinal motor neurons. Nature neuroscience. 11. 1122-4.

6. Arber, Silvia & Han, Barbara & Mendelsohn, Monica & Smith, Michael & Jessell, Thomas & Sockanathan, Shanthini. (1999). Requirement for the Homeobox Gene Hb9 in the Consolidation of Motor Neuron Identity. Neuron. 23. 659-74.

7. Bayraktar OA, Fuentealba LC, Alvarez-Buylla A, Rowitch DH. Astrocyte development and heterogeneity. Cold Spring Harb Perspect Biol. 2014 Nov 20;7(1):a020362.

8. Beaudet MJ, Yang Q, Cadau S, Blais M, Bellenfant S, Gros-Louis F, Berthod F. High yield extraction of pure spinal motor neurons, astrocytes and microglia from single embryo and adult mouse spinal cord. Sci Rep. 2015 Nov 18;5:16763.

9. Dasen JS, De Camilli A, Wang B, Tucker PW, Jessell TM. Hox repertoires for motor neuron diversity and connectivity gated by a single accessory factor, FoxP1. Cell. 2008 Jul 25;134(2):304-16.

10. Dasen JS, Tice BC, Brenner-Morton S, Jessell TM. A Hox regulatory network establishes motor neuron pool identity and target-muscle connectivity. Cell. 2005 Nov 4;123(3):477-91.

11. Deneen, B., Ho, R., Lukaszewicz, A., Hochstim, C., Gronostajski, R., Anderson, D., 2007. The Transcription Factor NFIA Controls the Onset of Gliogenesis in the Developing Spinal Cord. Neuron. 52. 953-68.

12. Glasgow, S., Carlson, J., Zhu, W., Chaboub, L., Kang, P., Lee, H.K., Clovis, Y.M., Lozzi, B., McEvilly, R., Rosenfeld, M., Creighton, C., Lee, S.K., Mohila, C., Deneen, B., 2017. Glia-specific enhancers and chromatin structure regulate NFIA expression and glioma tumorigenesis. Nature Neuroscience. 20.

13. Glasgow, S., Laug, D., Brawley, V., Zhang, Z., Corder, A., Yin, Z., Wong, S., Li, X., Foster, A., Ahmed, N., Deneen, B., 2013. The miR-223/Nuclear Factor I-A Axis Regulates Glial Precursor Proliferation and Tumorigenesis in the CNS. The Journal of neuroscience : the official journal of the Society for Neuroscience. 33. 13560-13568.

14. Gogliotti, Rocky & Quinlan, Katharina & Barlow, Courtenay & Heier, Christopher & Heckman, Cj & Didonato, Christine. (2012). Motor Neuron Rescue in Spinal Muscular Atrophy Mice Demonstrates That Sensory-Motor Defects Are a Consequence, Not a Cause, of Motor Neuron Dysfunction. The Journal of neuroscience : the official journal of the Society for Neuroscience. 32. 3818-29.

15. Gronostajski, Richard. 2000. Roles of the NFI/CTF gene family in transcription and development. Gene. 249. 31-45.

16. Hermann, Petra & Logan, C. (2003). Electroporation of proviral RCAS DNA alters gene expression in the embryonic chick hindbrain. BioTechniques. 35. 942-6, 948.

17. Huang AY, Woo J, Sardar D, Lozzi B, Bosquez Huerta NA, Lin CJ, Felice D, Jain A, Paulucci-Holthauzen A, Deneen B. Region-Specific Transcriptional Control of Astrocyte Function Oversees Local Circuit Activities. Neuron. 2020 Jun 17;106(6):992-1008.e9.

18. Kang P, Lee HK, Glasgow SM, Finley M, Donti T, Gaber ZB, Graham BH, Foster AE, Novitch BG, Gronostajski RM, Deneen B. Sox9 and NFIA coordinate a transcriptional regulatory cascade during the initiation of gliogenesis. Neuron. 2012 Apr 12;74(1):79-94.

19. Kania A, Johnson RL, Jessell TM. Coordinate roles for LIM homeobox genes in directing the dorsoventral trajectory of motor axons in the vertebrate limb. Cell. 2000 Jul 21;102(2):161-73.

20. Laug, D., Glasgow, S., Deneen, B., 2018. A glial blueprint for gliomagenesis. Nature Reviews Neuroscience. 19. 1.

21. Lee SK, Lee B, Ruiz EC, Pfaff SL. Olig2 and Ngn2 function in opposition to modulate gene expression in motor neuron progenitor cells. Genes Dev. 2005 Jan 15;19(2):282-94.

22. Liang, Xingqun & Song, Mi-Ryoung & Xu, ZengGuang & Lanuza, Guillermo & Liu, Yali & Zhuang, Tao & Chen, Yihan & Pfaff, Samuel & Evans, Sylvia & Sun, Yunfu. (2011).

Isl1 Is required for multiple aspects of motor neuron development. Molecular and cellular neurosciences. 47. 215-22.

23. Louis Sam Titus ASC, Yusuff T, Cassar M, Thomas E, Kretzschmar D, D'Mello SR. Reduced Expression of Foxp1 as a Contributing Factor in Huntington's Disease. J Neurosci. 2017 Jul 5;37(27):6575-6587.

24. Mason, S., Piper, M., Gronostajski, R., Richards, L., 2002. Nuclear factor one transcription factors in CNS development. Molecular Neurobiology. 39 (1): 10-23.

25. Pfaff SL, Mendelsohn M, Stewart CL, Edlund T, Jessell TM. Requirement for LIM homeobox gene Isl1 in motor neuron generation reveals a motor neuron-dependent step in interneuron differentiation. Cell. 1996 Jan 26;84(2):309-20.

26. Price SR, Briscoe J. The generation and diversification of spinal motor neurons: signals and responses. Mech Dev. 2004 Sep;121(9):1103-15.

27. Ravanelli AM, Appel B. Motor neurons and oligodendrocytes arise from distinct cell lineages by progenitor recruitment. Genes Dev. 2015 Dec 1;29(23):2504-15.

28. Rosenberg, Alexander & Roco, Charles & Muscat, Richard & Kuchina, Anna & Sample, Paul & Yao, Zizhen & Gray, Lucas & Peeler, David & Mukherjee, Sumit & Chen, Wei & Pun, Suzie & Sellers, Drew & Tasic, Bosiljka & Seelig, Georg. (2018). Single-cell profiling of the developing mouse brain and spinal cord with split-pool barcoding. Science. 360.

29. Shu T, Butz KG, Plachez C, Gronostajski RM, Richards LJ. Abnormal development of forebrain midline glia and commissural projections in Nfia knock-out mice. J Neurosci. 2003 Jan 1;23(1):203-12.

30. Stifani, Nicolas. 2014. Motor neurons and the generation of spinal motor neuron diversity. Frontiers in cellular neuroscience. 8. 293.

31. Tanabe, Yasuto & William, Christopher & Jessell, Thomas. (1998). Specification of Motor Neuron Identity by the MNR2 Homeodomain Protein. Cell. 95. 67-80.

32. Thaler, Joshua & Lee, Soo-Kyung & Jurata, Linda & Gill, Gordon & Pfaff, Samuel. (2002). LIM Factor Lhx3 Contributes to the Specification of Motor Neuron and Interneuron Identity through Cell-Type-Specific Protein-Protein Interactions. Cell. 110. 237-49.

33. Zuchero, J. Bradley & Barres, Ben. (2015). Glia in mammalian development and disease. Development (Cambridge, England). 142. 3805-3809.